

**Anonymous Referee #1** (Review comments in regular; response in bold.)

General Comments:

The authors are thanked for their detailed and informative answers/results regarding the questions asked by this reviewer (in both the initial review and in the “2nd review” or “addendum”). Regarding the answer to the first question, the answer makes sense provided pre-existing ice was assumed in all simulations shown in Fig. 1 of the author responses (the response seemed to imply that pre-existing ice was assumed).

**Answer: Yes, all simulations included the effect from pre-existing ice in the ice nucleation parameterization.**

The only outstanding issue concerns the 3rd answer from the authors that concerns the assumption of pre-existing ice. It is fine to make this assumption as many other investigators are doing so, but since the paper is focused on TTL cirrus, the paper should include some explanation on why it makes sense to assume pre-existing ice in the case of TTL cirrus. This is particularly important since TTL cirrus are generally above the zone of anvil cirrus and residual ice crystals from decaying anvils should not generally be a source of pre-existing ice in TTL cirrus. So from where does this pre-existing ice affecting TTL cirrus come from?

**Answer: We thank the reviewer for detailed question and some suggested answers to the question. The question has been focused on the origin of the pre-existing ice in cirrus clouds in the TTL. Here we attempt to clarify how the ice nucleation parameterization is implemented in the GCM (CAM5 here) in our study and why it is important to include the effect from pre-existing ice. At each model step (or every 30 min), air conditions (T, RH, aerosols, etc.) are judged to see if new ice nucleation could occur in existing clouds (in the cloudy sky portion of the grid) or in newly formed clouds (in the clear sky portion of a grid). The inclusion of the pre-existing ice in the ice nucleation parameterization does not mean pre-existing ice is always there. New cirrus clouds can still form under clear-sky conditions without pre-existing ice. By including pre-existing clouds, which can be anvil cirrus at some altitudes and advected cirrus formed by large-scale uplift of air masses at others, the model includes the effect of the deposition of water vapor onto pre-existing ice particles in the cloudy portion of the grid. By doing this, the model can avoid artificial ice nucleation events in pre-existing ice clouds. This is illustrated in the following figure copied from Shi et al. (2015) who followed the evolution of a cirrus cloud with and without the consideration of pre-existing ice in the ice nucleation scheme. The model does not distinguish the origin of the pre-existing ice. So the pre-existing ice could be generated in-situ from previous time steps, advected from adjacent grid boxes, or can descend from upper grid boxes. The notion of “pre-existing” applies not only to the time step before the formation of new clouds but also to time steps prior to the previous model time step, if the clouds so formed are still present. Considering the relatively long lifetime of cirrus clouds in the TTL (days) compared to the model time step (30 min), the latter situation (previous model time steps) is quite common.**

**We included above information to more fully explain these processes in the revised manuscript.**

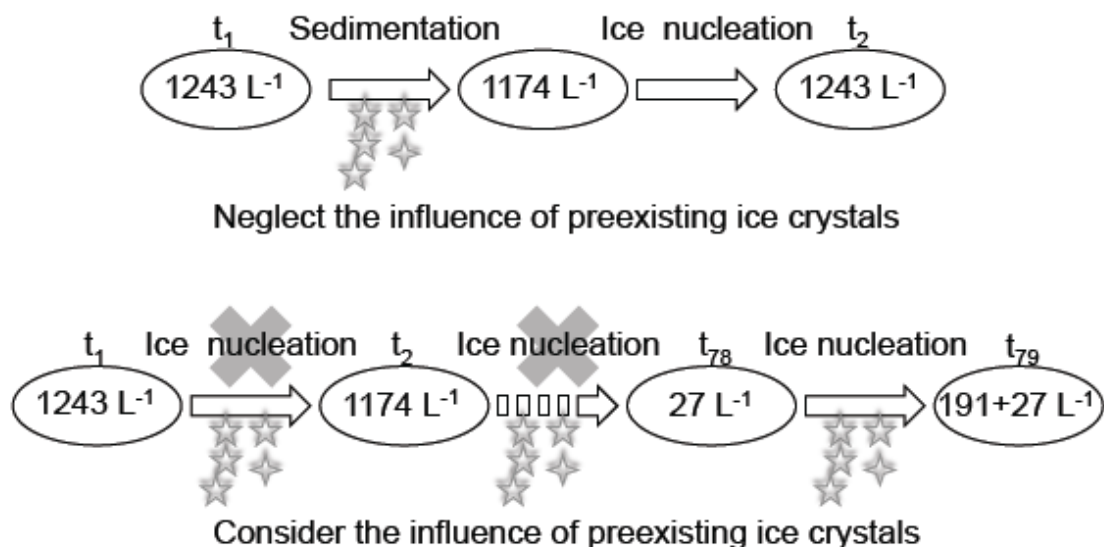


**Figure 2.** Schematic diagram of cirrus cloud evolution. Upper panel represents the default ice nucleation scheme that neglects the influence of PREICE; lower panel represents the updated scheme that considers the PREICE effect. Ice crystal number concentrations are shown inside the ovals. Time steps are shown above the ovals. All numbers are based on cirrus cloud evolution within a model grid cell ( $3^{\circ}$  N,  $75^{\circ}$  W,  $\sim 198$  hPa,  $\sim 217$  K). In this experiment, the updraft velocity is set to  $0.2 \text{ m s}^{-1}$  and the sulfate number concentration is set to  $100 \text{ cm}^{-3}$ . Heterogeneous nucleation is not taken into account. The simulation is run 3 months. Just one cirrus cloud evolution process is shown here.

In specific response to the 3rd answer from the authors regarding the initial review, it should be noted that in Diao et al. (2015), the ice nucleation zone was generally at the thermal tropopause, or just above it (e.g. see Fig. 13). The author's argument that ice crystals were advected into the nucleation zone from adjacent cirrus that were not sampled (in the Diao et al. study), thus introducing "pre-existing ice" into the nucleation zone (or adjacent cirrus advecting ice into an ISSR, creating an "apparent" nucleation zone), appears to be a weak argument. As the in situ measurements in Diao et al. (2015) show, there were no cirrus above the ice nucleation zone (i.e. above the thermal tropopause). For ice to be advected into the nucleation zone, it would need to be advected primarily from regions below the tropopause, which appears rather unlikely. Although the tropopause height varies in relation to distance from the jet core, upper troposphere winds follow the isobars and it is thus not likely for ice to advect from a higher to lower altitude along this tropopause surface. For the in situ cirrus sampled in Diao et al. (GRL 2013, 2014; JGR 2015), the pre-existing ice assumption is not well supported. While the nucleation zone was generally at the tropopause in Diao et al. (2015), there were a number of exceptions to this, and for those cases pre-existing ice appears somewhat more likely for the reasons the authors have mentioned.

**Answer:** Again we want to clarify the notion of “pre-existing” does not mean there is the always pre-existing ice for newly formed cirrus clouds in the TTL. Moreover, even if the reviewers’ contention that the cirrus observed by Diao et al were not from pre-existing ice is true, this does not mean that pre-existing ice never occurs. The parameterization in our model is meant to account for pre-existing ice, if and when it occurs. In the TTL, cirrus clouds can cover more than one grid box and can be advected horizontally across model grid boxes easily due to the horizontal wind. We do not agree that advection of pre-existing ice below the tropopause is necessarily unlikely. We argue that it is important to include the pre-existing ice effect when ice particles are advected from adjacent model grid boxes to ISS regions. When this occurs, the effect is included in the model. If it never occurs, the model accounts for nucleation in an ice-free region.

The pre-existing ice assumption does appear valid for liquid origin cirrus as described in Krämer et al. (ACP, 2016) and Luebke et al. (ACPD, 2015). These cirrus form as liquid cloud droplets from lower levels are advected into and freeze in the “cirrus zone” ( $T < 235$  K) via a conveyor belt of rising air associated with mid-latitude frontal systems or via strong updrafts associated with deep convection (i.e. anvil cirrus). It is very likely that ice crystals produced by these freezing cloud droplets will vigorously compete for water vapor among pre-existing ice particles. Under such conditions heterogeneous ice nucleation (het) should be strongly favored. Het may also dominate in most in situ cirrus, but perhaps not due to pre-existing ice.

**Answer:** We agree with the reviewer that the pre-existing ice can be transported from lower levels via a conveyor belt of rising air associated with mid-latitude frontal systems or via strong updrafts associated with deep convection. The occurrence frequency of heterogeneous nucleation depends on many factors including updraft velocity, IN numbers as well as pre-existing ice.

**Final recommendation:** Although the authors and this reviewer may differ on the pre-existing ice assumption, this paper is still a valuable study worthy of publication in ACP.

**Anonymous Referee #2** (Review comments in regular; response in bold.)

General comment:

The manuscript has improved in the revised version. However, some of my comments were not addressed sufficiently, thus I would suggest to consider these issues before the manuscript can be accepted. These issues are marginal and do not affect the whole qualitative and quantitative statements of the manuscript. Therefore, I recommend minor revisions, before the manuscript should be accepted.

Turbulence scheme:

As far as I understood the description of the scheme by Bretherton and Park (2009), it was developed for a better representation of the boundary layer. It is completely unclear how the scheme will behave in upper levels of the troposphere, since it was not developed for treating such thick layers in a much more stable environment. As far as I know, the behaviour of the scheme in the upper troposphere was not tested. Thus, the scheme might produce meaningful results but due to the wrong reasons. I understand that a detailed analysis of the scheme is beyond the scope of the manuscript, but I would like to see a more concrete statement about the uncertainty of the turbulence scheme.

**Answer: We agree with the reviewer that the behaviour of the moist turbulence scheme in the upper troposphere was not well tested. However, the updraft velocity (WSUB) in the upper troposphere based on the TKE from this scheme agrees reasonably well with aircraft measurements from the SPARTICUS campaign though it was limited in time and location (near 36.6N, 97.5W). Below is a graph copied from Fig 3 of Shi et al. (2015) which shows the PDFs of WSUB from the observations and different CAM5 simulations. The “Preice” case is similar to the pre-existing ice cases in this study. Overall the PDF from the “Preice” case agrees reasonably well with the observations.**

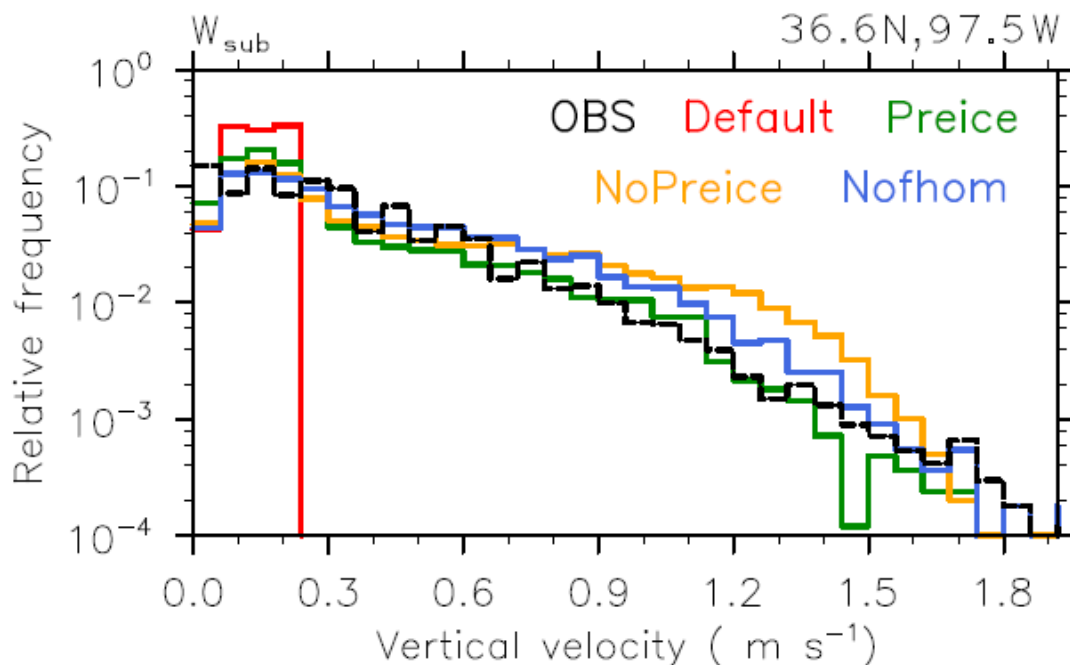


Figure 1. Probability distribution frequency of sub-grid updraft velocity ( $W_{sub}$ ) for Default, Preice, Nofhom and NoPreice experiments. Black dashed line refers to aircraft **However, other measurements from superpressure balloons near the equator reported in Podglajen et al. (2016) suggest WTKE may be overestimated.**

**We added this information in the revised manuscript:**

*“Since the Bretherton and Park (2009) scheme was initially developed for a better representation of the boundary layer, it is not clear how accurate the calculated WTKE is for the upper levels of the troposphere. Probability density functions of WTKE in the upper troposphere were previously compared to aircraft measurements from the SPARTICUS campaign (Shi et al. 2015) and show overall agreement although the comparison was limited in time and location. Fig. 1a shows that WTKE has the largest range of the three representations. It has a spike near zero which occurs when strong turbulence/convection is absent in a grid. The remaining portion of the PDF has a wide range from 0 to 2 m s<sup>-1</sup>. A recent study by Podglajen et al. (2016) shows that the updraft velocity from superpressure balloon measurements in equatorial regions has a characteristic value of 0.11-0.46 m s<sup>-1</sup> depending on the chosen frequency range. This suggests the calculated WTKE in the model may be at the upper end of observed updrafts compared to observations (see Fig. 2d in Podglajen et al. 2016).”*

**WGARY:**

I do not agree that the results from the WGARY parameterization in fig. 4(b) are convincing, since in the high temperature regime ( $T > 210$  K) there is almost no variability. From this perspective it seems that the WGARY scheme is the weakest parameterization, especially because it is only depending on mean values of pressure, topography and latitude but does not take into account dynamic and convective instabilities, i.e. the actual state of the atmosphere.

**Answer:**

**We added the following in Section 3.1 in the revised manuscript:**

*“The overall wave amplitude using the Gary scheme is at the low end compared to other aircraft or superpressure balloon measurements (Kärcher and Ström, 2003; Podglajen et al. 2016).”*

**We added the following in Section 3.3 in the revised manuscript:**

*“Caution is needed in interpreting these results. Due to the possible underestimate of subgrid updraft velocities in the upper troposphere when using WGARY (as discussed in Section 3.1) and its oversimplified fitting which does not take into account the time-varying state of the atmosphere, this scheme might be considered a somewhat weaker parameterization than one that accounts for the full variability of the background atmospheric state. As a result, the simulated ice numbers are only statistically meaningful for mean climate states.”*

**Added Reference**

Podglajen, A., A. Hertzog, R. Plougonven, and B. Legras (2016), Lagrangian temperature and vertical velocity fluctuations due to gravity waves in the lower stratosphere, *Geophys. Res. Lett.*, 43, 3543–3553, doi:10.1002/2016GL068148.

# 1 What Controls the Low Ice Number Concentration in the 2 Upper Troposphere?

3 C. Zhou<sup>1</sup>, J. E. Penner<sup>1</sup>, G. Lin<sup>1\*</sup>, X. Liu<sup>2</sup> and M. Wang<sup>3,4</sup>

4 (1){University of Michigan, Ann Arbor, MI, USA}

5 (2){University of Wyoming, Laramie, WY, USA}

6 (3) {Institute for Climate and Global Change Research & School of Atmospheric Sciences,  
7 Nanjing University, Nanjing, 210023, China}

8 (4) {Collaborative Innovation Center of Climate Change, Jiangsu Province, China}

9  
10 (\*){now at: Pacific Northwest National Laboratory, Richland, Washington, USA}

11 Correspondence to: C. Zhou (zhouc@umich.edu)

## 12 13 Abstract

14 Cirrus clouds in the tropical tropopause play a key role in regulating the moisture  
15 entering the stratosphere through their dehydrating effect. Low ice number concentrations  
16 ( $<200 \text{ L}^{-1}$ ) and high supersaturations (150-160%) have been observed in these clouds.  
17 Different mechanisms have been proposed to explain these low ice number concentrations,  
18 including the inhibition of homogeneous freezing by the deposition of water vapour onto pre-  
19 existing ice crystals, heterogeneous ice formation on glassy organic aerosol ice nuclei (IN),  
20 and limiting the formation of ice number from high frequency gravity waves. In this study, we  
21 examined the effect from three different representations of updraft velocities, the effect from  
22 pre-existing ice crystals, the effect from different water vapour deposition coefficients ( $\alpha=0.1$   
23 or 1), and the effect of 0.1% of the total secondary organic aerosol (SOA) particles acting as  
24 IN. Model simulated ice crystal numbers are compared against an aircraft observational  
25 dataset.

26 Including the effect from water vapour deposition on pre-existing ice particles can  
27 effectively reduce simulated in-cloud ice number concentrations for all model set-ups. A  
28 larger water vapour deposition coefficient ( $\alpha=1$ ) can also efficiently reduce ice number  
29 concentrations at temperatures below 205K but less so at higher temperatures. SOA acting as

1 IN are most effective at reducing ice number concentrations when the effective updraft  
2 velocities are moderate ( $\sim 0.05\text{--}0.2\text{ m s}^{-1}$ ). However, the effects of including SOA as IN and  
3 using ( $\alpha=1$ ) are diminished when the effect from pre-existing ice is included.

4 When a grid resolved large-scale updraft velocity ( $<0.1\text{ m s}^{-1}$ ) is used, the ice nucleation  
5 parameterization with homogeneous freezing only or with both homogeneous freezing and  
6 heterogeneous nucleation is able to generate low ice number concentrations in good  
7 agreement with observations for temperatures below 205K as long as the pre-existing ice  
8 effect is included. For the moderate updraft velocity ( $\sim 0.05\text{--}0.2\text{ m s}^{-1}$ ) simulated ice number  
9 concentrations in good agreement with observations at temperatures below 205K can be  
10 achieved if effects from pre-existing ice, a larger water vapour deposition coefficient ( $\alpha=1$ )  
11 and SOA IN are all included. Using the sub-grid scale turbulent kinetic energy based updraft  
12 velocity ( $\sim 0\text{--}2\text{ m s}^{-1}$ ) always overestimates the ice number concentrations at temperatures  
13 below 205K but compares well with observations at temperatures above 205K when the pre-  
14 existing ice effect is included.

15

## 16 **1 Introduction**

17 Cirrus clouds ( $T < 35\text{ }^\circ\text{C}$ ) cover about a large fraction of the Earth's area from more than  
18 10% to more than 30% depending on observational times, techniques and different thresholds  
19 of detectable optical depth (Wang et al., 1996; Rossow and Schiffer, 1999; Wylie and Menzel,  
20 1999; Stubenrauch et al. 2000; Sassen et al., 2008) and are important in maintaining the  
21 global radiation balance (Ramanathan and Collins, 1991). They warm the atmosphere by  
22 absorbing outgoing longwave radiation emitted by the Earth and atmosphere and re-emitting  
23 it at much lower temperatures. This warming effect is partly compensated by their reflection  
24 of incoming solar radiation (Chen et al. 2000; IPCC 2013). Cirrus clouds also control the  
25 dehydration of air before its entry into the stratosphere (Jensen et al., 1996, 2013). Their  
26 radiative impacts, ability to affect water vapour cycles, and cirrus cloud evolution are  
27 sensitive to the ice number concentration. Ice in cirrus clouds can form through either  
28 homogeneous freezing of supercooled aqueous solutions (Koop et al. 2000) which typically  
29 generates high ice number concentrations or heterogeneous nucleation of different modes  
30 (deposition, contact, immersion, and condensation) triggered by insoluble aerosol particles  
31 (which are termed heterogeneous ice nuclei (IN)) (Pruppacher and Klett, 1997).

1 Heterogeneous nucleation typically forms much lower ice number concentrations due to the  
2 limited IN concentration in the atmosphere (Rogers et al. 1998).

3 Low ice number concentrations ( $<200 \text{ L}^{-1}$ ) and high in-cloud ice supersaturations (RH<sub>i</sub>)  
4 (150-160%) are frequently observed near the tropical tropopause layer (TTL) (e.g. Krämer et  
5 al., 2009; Jensen et al. 2010, 2013). The observed high in-cloud ice supersaturations are  
6 consistent with the long relaxation times needed to remove the excess water vapour above ice  
7 saturation by deposition due to low ice number concentrations. These low ice numbers are not  
8 consistent with the conventional theory of ice nucleation via homogenous freezing at the cold  
9 temperatures in the TTL (e.g. Krämer et al., 2009; Jensen et al. 2010) if a typical value of  
10 temperature fluctuation or updraft velocity is used.

11 Various proposals have been put forward to explain the low ice number concentrations in  
12 the TTL. These can largely be divided into 3 categories. The first category is inhibition of  
13 homogeneous freezing by heterogeneous IN (e.g. Abbatt et al. 2006; Murray et al. 2010) or  
14 pre-existing ice particles (e.g. Kuebbeler et al. 2014; Shi et al. 2015). Abbatt et al. (2006)  
15 showed that solid ammonium sulphate aerosols can be effective heterogeneous ice nuclei at  
16 cirrus temperatures and lead to fewer but larger ice crystals compared to a homogeneous  
17 freezing scenario. Murray et al. (2010) showed that organic matter can become glassy under  
18 cirrus conditions and thereby become heterogeneous IN. Thus the low ice number and high  
19 RH<sub>i</sub> could be explained by heterogeneous nucleation of ice on glassy solution droplets.  
20 Kuebbeler et al. (2014) studied the effect of vapour deposition onto pre-existing ice during  
21 nucleation, which can prevent high supersaturations and thereby prevent either homogeneous  
22 or heterogeneous freezing from occurring. They found that the effect of pre-existing ice  
23 together with heterogeneous nucleation on mineral dust particles can significantly reduce  
24 global ice crystal number and mass. Shi et al. (2015) also found that the inclusion of vapour  
25 deposition onto pre-existing ice during nucleation significantly reduces ice number  
26 concentrations in cirrus clouds, especially at middle to high latitudes in the upper troposphere  
27 (by a factor of ~10).

28 The second category of proposals that might explain the observed low ice number  
29 concentrations in the TTL is related to gravity wave cycles (e.g. Spichtinger and Krämer  
30 2013; Dinh et al. 2015). In most ice nucleation parameterizations, it is often assumed that the  
31 relevant time scale for ice nucleation (i.e., a few minutes) is sufficiently short such that the  
32 vertical velocity and associated adiabatic cooling rate remain constant (e.g. Liu and Penner,



1 2005; Krächer et al., 2006; Barahona and Nenes, 2008). For the above proposals in the  
2 second category to form low ice numbers ( $<200 \text{ L}^{-1}$ ) the constant cooling rate or updraft  
3 velocity has to be low enough (several  $\text{cm s}^{-1}$ ). However, vertical velocity measurements from  
4 the Interhemispheric Differences in Cirrus Properties From Anthropogenic Emissions (INCA)  
5 campaign indicate that updraft velocities higher than  $0.2 \text{ m s}^{-1}$  are often observed (Krächer  
6 and Ström, 2003). Spichtinger and Krämer (2013) studied the effect of the superposition of a  
7 slow large-scale updraft with a high-frequency, short wavelength gravity wave. Under these  
8 circumstances, the observed TTL low cirrus ice numbers could be explained by “classical”  
9 homogeneous ice nucleation. They show model simulations of homogenous freezing starting  
10 at the tip of the high frequency wave just before it is about to turn from an upward movement  
11 to a downward movement. Consequently the amount of time available for homogenous  
12 freezing event is substantially limited due to the downdraft, and hence the newly formed ice  
13 number from homogeneous freezing is also reduced. They suggest that large-scale models  
14 would reproduce their results just by using the large-scale updraft velocity in ice nucleation  
15 parameterizations. Dinh et al. (2015) studied homogeneous ice nucleation using a parcel  
16 model with observed temperature time series from balloon flights near the tropical  
17 tropopause. They showed that low ice number concentrations can also be obtained if the  
18 gravity wave perturbations produce a non-persistent cooling rate such that the absolute change  
19 in temperature remains small during ice nucleation events.

20 The third category of proposals that might explain the observed low ice number  
21 concentrations in the TTL is related to the sedimentation of ice particles (e.g. Barahona and  
22 Nenes 2011; Murphy 2014). Barahona and Nenes (2011) showed that the dynamical balance  
23 between new ice particle production and sedimentation can set the cirrus clouds into one of  
24 two “preferred” microphysical regimes based on the magnitude of the temperature  
25 fluctuations. For small temperature fluctuations, the balance between the formation of ice  
26 crystals from homogeneous freezing and sedimentation was able to explain low ice number  
27 concentrations, although this finding could not be confirmed in the study by Jensen et al.  
28 (2012). Murphy (2014) showed that random temperature fluctuations can generate an  
29 extremely wide range of ice number densities. Since the low number density ice crystals are  
30 also associated with larger sizes, they sediment quickly and sweep out a much larger volume  
31 than that of the high number density ice crystals that stay aloft. Thus the rare temperature  
32 trajectories that result in the lowest number densities are disproportionately important. They

1 suggest the low mean and median observed ice number concentrations are caused by aircraft  
2 observations which usually measure low ice number density in this much larger volume.

3 In this study, we will examine the first two categories of proposals in a GCM to see if  
4 we are able to generate low ice number concentrations consistent with observations. We will  
5 not evaluate the third category related to ice sedimentation. Even though sedimentation of ice  
6 is included in the GCM (CAM5 in this study) by applying the mass- and number-weighted  
7 terminal fall speeds which are obtained by integration over the particle size distributions with  
8 appropriate weighting by number concentration or mixing ratio (Morrison and Gettelman  
9 2008), the vertical grid spacing (with 30 vertical layers) is not fine enough to capture the  
10 observed narrow layers of high ice crystal number concentrations with low ice crystal number  
11 concentration layers surrounding them (Jensen et al., 2013). For the first category of  
12 proposals, we will examine the effect of pre-existing ice and secondary organic aerosols  
13 (SOA) acting as IN. For the second category of proposals, we will examine three different  
14 representations of sub-grid updraft velocities in the ice nucleation parameterizations. For the  
15 first representation, we follow the suggestion by Spichtinger and Krämer (2013) and simply  
16 use the large-scale updraft velocity predicted by the GCM in the ice nucleation  
17 parameterization, excluding any effect from fast gravity waves. For the second representation,  
18 we use the sub-grid scale updraft velocity based on the fitted meso-scale temperature  
19 fluctuations from long-term aircraft temperature observations (Gary 2006, 2008). This sub-  
20 grid scale updraft velocity was first introduced in a GCM by Wang and Penner (2010) and  
21 further studied by Wang et al. (2014). Wang et al. (2014) showed that using this updraft  
22 velocity produces a better hemispheric contrast in ice supersaturation compared to  
23 observations. The third representation is the sub-grid scale updraft velocity based on the  
24 modelled sub-grid scale turbulent kinetic energy (TKE) (Neale et al. 2012; Gettelman et al.  
25 2010). As shown in Fig. 1, this updraft velocity has the largest range. We will also examine  
26 the effect of using different mass accommodation coefficients ( $\alpha$ ) for water vapour deposition  
27 on ice crystals. This coefficient is not well known but has a significant impact on the  
28 predicted ice numbers (Zhang et al. 2013; Murphy 2014). Laboratory measurements support  
29 values from 0.006 (Magee et al. 2006) to unity (Skrotzki et al. 2013). Skrotzki et al. (2013)  
30 constrained the value in the range of 0.2-1 with the majority of other lab studies also  
31 supporting a value  $> 0.1$  (see Table 1 in Skrotzki et al. (2013)). Kay and Wood (2008) showed  
32 that  $\alpha$  is  $\geq 0.1$  for small ice crystals forming at high ice supersaturations, so the small value of  
33  $\alpha$  ( $=0.006$ ) from (Magee et al., 2006) may only be appropriate for large ice crystals or at low

1 ice supersaturations. In this study we test two values of  $\alpha$  (0.1 and 1). The model and  
2 experiments are described in section 2. Model results are presented in section 3. Section 4  
3 presents a summary and a short discussion.

## 4 **2 Model and Experiments**

### 5 **2.1 Description of the coupled CAM5/IMPACT model**

6 We used the coupled CAM5/IMPACT model in this study. The CAM5/IMPACT model  
7 embeds the University of Michigan IMPACT chemistry and aerosol transport model as a  
8 module inside the Community Atmosphere Model version 5.3 (CAM5) (Zhou and Penner  
9 2014). CAM5 is the atmospheric component of the Community Earth System Model version  
10 1.2 (CESM1.2). Readers are referred to Neale et al. (2012) and Liu et al. (2012a) for more  
11 model details. Here we briefly summarize the ice nucleation process. Observation-based  
12 studies (e.g., Diao et al. 2013, 2014, 2015) as well as modelling studies (e.g., Spichtinger and  
13 Gierens 2009) show that the evolution of cirrus clouds undergo different phases including a  
14 clear-sky phase, ice nucleation phase, growth phase and decaying phase. Diao et al. (2013)  
15 suggests that the ice nucleation phase is a short-lived transient event since only 3-4% of  
16 sampled events are in this phase. GCMs (CAM5 here) usually use the time step longer than  
17 the duration of an ice nucleation event (30 min here). Thus the ice nucleation process has to  
18 be parameterized. The default ice nucleation scheme for cirrus clouds (below  $-35\text{ }^{\circ}\text{C}$ ) in  
19 CAM5 follows the parameterization developed by Liu and Penner (2005) (hereafter LP) and  
20 was implemented in CAM3 by Liu et al. (2007) and later in CAM5 by Gettelman et al.  
21 (2010). The LP parameterization treats the competition between homogenous freezing on  
22 sulphate haze droplets and heterogeneous nucleation on dust as well as other IN. Shi et al.  
23 (2015) included the effect of deposition of water vapour onto pre-existing ice in ice nucleation  
24 using the LP parameterization. The pre-existing ice could be generated in-situ from previous  
25 time steps, advected horizontally from adjacent grid boxes, descend from upper grid boxes, or  
26 can be transported from lower levels via a conveyer belt of rising air associated with mid-  
27 latitude frontal systems or via strong updrafts associated with deep convection. The notion of  
28 “pre-existing” applies not only to the time step before the formation of new clouds but also to  
29 time steps prior to the previous model time step, if the clouds so formed are still present. By  
30 including this effect from pre-existing ice, the model can avoid artificial ice nucleation events  
31 in these pre-existing ice clouds. The CAM5 model has also been expanded to include ~~We~~  
32 also tested the ice nucleation parameterization by Barahona and Nenes (2009) (hereafter BN).

1 In this study, we used both parameterizations. The BN parameterization has the flexibility to  
2 use different water accommodation coefficients and different ice nucleation parameterizations  
3 for heterogeneous nucleation including those in Meyers et al. (1992), Phillips et al. (2007) and  
4 Phillips et al. (2008) as well as the classical-nucleation-theory (CNT) (see Table 1 in  
5 Barahona and Nenes (2009)). The LP parameterization used the CNT based IN mechanism  
6 only and a fixed water accommodation coefficient equal to 0.1. To facilitate the comparison  
7 between the two parameterizations, we chose to use the CNT based IN mechanism in BN. In  
8 both ice nucleation parameterizations, up to 100% of the potential IN are allowed to freeze  
9 when criteria for temperatures and supersaturations are met. The results from the LP  
10 parameterization are very similar to the results from the BN parameterization when the water  
11 vapour accommodation coefficient is set to 0.1. So we only present the results from the BN  
12 parameterization here.

13 The IMPACT module runs in parallel with the default CAM5 aerosol module (MAM3)  
14 in CAM5 (Zhou and Penner 2014). Aerosols simulated by the IMPACT module do not  
15 interact with any physical processes in CAM5 except in cirrus clouds (below -35 °C). In the ice  
16 nucleation parameterization sulphate particles and heterogeneous IN predicted by IMPACT  
17 replace those predicted by MAM3. The performance of the offline IMPACT model driven by  
18 CAM5 meteorological fields was previously evaluated by Zhou et al. (2012a, 2012b) and was  
19 in good agreement with observations. The overall characteristics of the performance of the  
20 coupled IMPACT module within CAM5 are similar to this offline version. We present  
21 simulations using two versions of IMPACT, the basic version without secondary organic  
22 aerosols (SOA) and the version that includes SOA. The basic version simulates a total of 17  
23 externally mixed aerosol types and/or size bins: 3 sizes representing the number and mass of  
24 pure sulphate aerosols (i.e. nucleation, Aitken and accumulation modes), 3 types of fossil/bio-  
25 fuel soot that depend on its hygroscopicity or the amount of sulphate on the soot particles, 2  
26 aircraft soot modes (pre-activated in contrails or not), 1 biomass soot mode, 4 dust sizes, and  
27 4 sea salt sizes. All these aerosols may mix with sulphate through condensation and  
28 coagulation processes or through sulphate formation in cloud drops. Thus, for all non-sulphate  
29 aerosols we also track the amount of sulphate mass coated on them. The SOA version  
30 includes the volatile organic compound (VOC) oxidation scheme implemented in *Lin et al.*  
31 (2012, 2014). It has approximately 129 separate gas-phase compounds (depending on which  
32 chemical oxidation scheme is used). It uses a chemical mechanism that includes both gas  
33 phase and aqueous or liquid phase production of SOA. Specifically, Glyoxal and

1 methylglyoxal are dissolved into cloud and aqueous sulfate to form SOA, and some SOA is  
2 formed through the reactive uptake of epoxides on aqueous sulfate. Twenty different semi-  
3 volatile organic compounds (SVOCs), mainly consisting of organic nitrates and peroxides that  
4 are formed from gas phase VOC oxidations, are partitioned into the aerosol phase. In  
5 addition, when present within the aerosol phase, the SVOCs form oligomers using a  
6 simplified scheme (*Lin et al.*, 2012). In total, in addition to the 17 aerosol species in the basic  
7 version of IMPACT described above, the *Lin et al.* (2014) version separately follows a total  
8 of 35 additional low-volatility SOA species.

## 9 **2.2 Experiment Description**

10 In the ice nucleation parameterization, we specify a single updraft velocity at each grid  
11 point. We used three different representations of the updraft: the grid resolved updraft  
12 velocity (WGRID), the updraft velocity derived from observed meso-scale temperature  
13 fluctuations as summarized by Gary (2006, 2008) (WGARY), and the updraft velocity based  
14 on the modelled sub-grid scale turbulent kinetic energy (WTKE). For each updraft  
15 representation, we used 4 different model set-ups, depending on whether heterogeneous  
16 nucleation (COMP), vapour deposition on pre-existing ice during ice nucleation (PRE), or  
17 SOA IN (SOA01) are included in the ice nucleation parameterization (COMP,  
18 COMP+SOA01, COMP+PRE and COMP+PRE+SOA01). Table 1 gives the definition of the  
19 set-ups for each updraft velocity category. In addition, for WGRID we added 2 other set-ups:  
20 a case with only homogeneous nucleation allowed (HOM) and a model set-up with vapour  
21 deposition on pre-existing ice during ice nucleation (HOM+PRE). Since we also vary the  
22 water vapour accommodation coefficient ( $\alpha=0.1$  or  $\alpha=1$ ), each set-up also includes a pair of  
23 simulations, one with  $\alpha=0.1$  and one with  $\alpha=1$ . All cases use a horizontal resolution of  
24  $2.5^\circ \times 1.9^\circ$  and 30 vertical layers and are run for 6 years using year 2000 emissions. We chose  
25 to run the SOA capable version of the CAM/IMPACT model for only 2 years and to read-in  
26 the stored monthly averaged SOA fields from the second year for all cases, since the SOA  
27 capable version of the CAM/IMPACT model takes roughly 1.5 times more computer time  
28 than the basic version. The use of monthly averaged SOA fields does not significantly change  
29 the nature of the results. The output from the last 5 years of each simulation case is used in the  
30 analysis.

## 1 **3 Results**

### 2 **3.1 Updraft velocities and SOA IN numbers**

3 The updraft velocity plays a crucial role in ice nucleation. It determines how fast the  
4 RHi can grow and thus determines whether the RHi reaches the threshold for ice nucleation to  
5 occur after vapour deposition on newly formed ice begins. Figure 1a shows the probability  
6 density functions (PDFs) determined by sampling the updraft used during nucleation over  
7 tropical grids. Model results are sampled every 3 hours from all grid points between 30 S to  
8 30 N and below 87hPa. The PDFs for the three different updraft velocities used here are  
9 shown for two different temperature ranges (185K-205K and 205K-225K). Results are from  
10 the COMP case in each updraft velocity category with  $\alpha=0.1$ . The grid resolved large scale  
11 updraft velocity (WGRID) shows both negative and positive values varying between about -  
12  $0.05 \text{ m s}^{-1}$  to  $0.15 \text{ m s}^{-1}$ . The magnitude of WGRID decreases as the temperature decreases  
13 (from 205K-225K to 185K-205K) or when the altitude increases. WGARY is the updraft  
14 velocity derived from the observed meso-scale temperature fluctuations,  $\delta T$ , and is a function  
15 of altitude, topography, season, and latitude (Gary 2006, 2008). The observed temperature  
16 fluctuations were converted to sub-grid scale vertical velocities using

$$17 \quad WGARY \text{ (m s}^{-1}\text{)} = 0.23 \delta T \text{ (K)}$$

18 following Kärcher and Burkhardt (2008) (also see Wang and Penner 2010 and Wang et al.  
19 2014). WGARY varies from  $0.05 \text{ m s}^{-1}$  to  $0.15 \text{ m s}^{-1}$  and shows increased magnitudes as the  
20 temperature decreases with altitude. This increase is proportional to  $p^{-0.4}$  ( $p$  is the pressure, see  
21 equation 3 in Gary (2008)) and is similar to the increase caused by the increase in the wave  
22 amplitudes required to conserve wave energy when the air density decreases with altitude.  
23 The overall wave amplitude is at the low end compared to other aircraft or superpressure  
24 balloon measurements (Kärcher and Ström, 2003; Podglajen et al. 2016). WTKE is the  
25 updraft velocity calculated from the modelled sub-grid turbulent kinetic energy (TKE)  
26 following Morrison and Pinto (2005):

$$WTKE = \sqrt{\frac{2}{3} TKE}$$

27 The TKE is diagnosed from CAM5's moist turbulence scheme (Bretherton and Park, 2009),  
28 which simulates cloud-radiation-turbulence interactions in an explicit way and is operating in  
29 any layer above as well as within PBL as long as the moist Richardson number is larger than a

1 critical value, 0.19. Since the Bretherton and Park (2009) scheme was initially developed for  
2 a better representation of the boundary layer, it is not clear how accurate the calculated  
3 WTKE is for the upper levels of the troposphere. Probability density functions of WTKE in  
4 the upper troposphere were previously compared to aircraft measurements from the  
5 SPARTICUS campaign (Shi et al. 2015) and show overall agreement although the  
6 comparison was limited in time and location. Fig. 1a shows that WTKE has the largest range  
7 of the three representations. It has a spike near zero which occurs when strong  
8 turbulence/convection is absent in a grid. The remaining portion of the PDF has a wide range  
9 from 0 to 2 m s<sup>-1</sup>. A recent study by Podglajen et al. (2016) shows that the updraft velocity  
10 from superpressure balloon measurements in equatorial regions has a characteristic value of  
11 0.11-0.46 m s<sup>-1</sup> depending on the chosen frequency range. This suggests the calculated WTKE  
12 in the model may be at the upper end of observed updrafts compared to observations (see Fig.  
13 2d in Podglajen et al. 2016). Large updraft velocities, such as those at the higher end of this  
14 range produced from convection in the tropics, are accompanied by homogeneous freezing as  
15 we show later. Previously, an artificial upper limit of 0.2 m s<sup>-1</sup> was used for WTKE in ice  
16 nucleation studies using the CAM5 model (Gettelman et al. 2010, 2012; Liu et al. 2012b;  
17 Zhang et al. 2013) to better reproduce observed in-cloud ice number concentrations. This  
18 upper limit was removed by Shi et al. (2015) after adding vapour deposition on pre-existing  
19 ice during ice nucleation. Here we also use the predicted updraft based on the TKE without  
20 any upper limit. We note that Shi et al. (2015) also limited the fraction of each grid cell that  
21 was allowed to undergo homogenous freezing. Here, we do not add this constraint.

22 During in-cloud ice nucleation, the updraft velocity ( $W$ ) acts to increase the relative  
23 humidity by cooling the air parcel through adiabatic expansion while pre-existing ice particles  
24 act to decrease the relative humidity by consuming any water vapour above ice saturation. So  
25 mathematically, one can combine the effects of pre-existing ice particles and those from the  
26 cooling caused by the updraft velocity. This is equivalent to the use of a reduced updraft  
27 velocity while ignoring vapour deposition on pre-existing ice particles. This reduced updraft  
28 velocity is termed the effective updraft velocity (Kärcher et al. 2006; Shi et al. 2015). Figure  
29 1b shows the PDFs of the three different updraft velocities and their effective updraft  
30 velocities in the temperature range 185K-205K sampled from grid points that only experience  
31 homogenous freezing. The effective updraft velocities shift to the left towards the smaller  
32 values. The effective WGRID PDF now only shows positive values since homogeneous  
33 freezing only occurs in grid boxes with updrafts that are positive and are cooling. Although

1 the effective WTKE is significantly reduced, it still has a large fraction with values larger than  
2  $0.2 \text{ m s}^{-1}$ .

3 In addition to the important role that the updraft velocity plays in ice nucleation, the  
4 concentrations of heterogeneous IN also play an important role by determining the  
5 competition between heterogeneous nucleation and homogeneous freezing. However, our  
6 understanding of which aerosol particles may serve as heterogeneous IN is still limited  
7 (Hoose and Möhler, 2012) and even the importance of heterogeneous nucleation for the cold  
8 temperature regime (i.e.,  $T < 235 \text{ K}$ ) is still under discussion and not clear at the moment. The  
9 ability of different types of aerosols acting as IN was investigated in laboratory experiments  
10 (e.g., the formation of ice crystals on glassy particles). However, *in situ* measurements of  
11 heterogeneous IN are difficult. Furthermore, the existence of glassy particles within the  
12 atmosphere has not been established by *in situ* measurements. The field study by Cziczo et al.  
13 (2013) showed that mineral dust dominates most measurements of the residual particles in ice  
14 crystals. Another field study by Pratt et al. (2009) showed that ice-crystal residues from an  
15 aircraft measurement at high altitudes over Wyoming are comprised mostly of biological  
16 particles (~33%) and mineral dust (~50%) with some minor contribution from soot (~4%),  
17 salt (~4%) and organic carbon/nitrate (~9%). Moreover, the measurements in Cziczo et al.  
18 (2013) are mainly from convective regions in the subtropics and are certainly not  
19 representative for the whole upper troposphere, especially not for mid or high latitude  
20 conditions. Also the relevance of biological particles at cirrus level is not clear, since Pratt et  
21 al. (2009) could provide only one flight at about 7 kilometres (i.e. at temperatures  $T > 240 \text{ K}$ ),  
22 which is also not representative for the whole upper troposphere. Lab studies show that  
23 activated fractions of Asian and Saharan desert dust can range from ~5–10% at  $-20 \text{ }^\circ\text{C}$  to 20–  
24 40% at temperatures colder than  $-40 \text{ }^\circ\text{C}$  (Field et al. 2006). In this study we assumed that 10%  
25 of the total dust number can act as IN which is similar to the fractions suggested by Zhang et  
26 al. (2013) and Wang et al. (2014). For primary carbonaceous aerosols, we assume 0.1% of  
27 hydrophilic fossil fuel soot, 0.05% of hydrophobic fossil fuel soot (Koehler et al., 2009) and  
28 0.1% of total biomass burning soot (Möhler et al. 2005) are able to act as heterogeneous IN.  
29 For SOA, we lumped together all 35 SOA compounds together and assumed that 0.1% of the  
30 total SOA could act as IN, similar to the fraction of biomass burning soot.

31 Figure 2 shows the annual zonal mean sulphate aerosol number concentration above 500  
32 hPa in the Aitken and accumulation modes which are the number of particles able to freeze



1 homogeneously. The number concentrations for different heterogeneous IN are also shown.  
2 The simulated sulphate number in the Aitken and accumulation modes (fig. 2a) is of the order  
3 of  $100 \text{ cm}^{-3}$  in the tropical upper troposphere. The total IN without SOA (fig. 2b) ranges from  
4  $0.5$  to  $30 \text{ L}^{-1}$  in the upper troposphere. They are dominated by dust IN (fig. 2d) with a minor  
5 contribution from biomass burning soot (fig. 2e) below the tropopause. The contribution from  
6 fossil/bio fuel soot is even smaller and is largely negligible above 150 hPa. The number  
7 concentration of 0.1% of SOA, which we treat here as IN, ranges 1 to  $30 \text{ L}^{-1}$  in upper  
8 troposphere (fig. 2c) and is about 2-5 times larger than the total background IN number  
9 without SOA above 200 hPa, except in the dust source and outflow regions near north Africa  
10 (not shown).

### 11 **3.2 Results from WGRID cases**

12 In this section, we examine the effect from water vapour deposition on pre-existing ice  
13 particles on ice crystal number concentrations when the grid resolved updraft velocity  
14 (WGRID) is used in the ice nucleation parameterization. We also examine the effect of  
15 including SOA as IN and of varying the water vapour accommodation coefficient. The use of  
16 the large-scale updraft velocity during ice nucleation is based on the parcel model study by  
17 Spichtinger and Krämer (2013). They showed that the superposition of large-scale updrafts  
18 and fast gravity waves would limit the ice nucleation time duration and thus the ice number.  
19 They showed that about 80% of the observed ice spectrum could be explained by  
20 homogenous freezing while the remaining 20% stem from heterogeneous and homogeneous  
21 freezing occurring within the same environment, and suggested that their parcel model results  
22 could be reproduced using only the large-scale updraft velocity. Here we test this theory by  
23 using the large-scale grid resolved updraft velocity in the ice nucleation parameterization in  
24 CAM5.

25 Figure 3 shows the simulated in-cloud ice number concentrations as a function of  
26 temperature from the WGRID cases. The top panel shows the results from the homogeneous  
27 freezing only cases and bottom panel shows the results from the homogeneous  
28 freezing/heterogeneous nucleation competition cases. The left and right panels show the  
29 results using two different water vapour accommodation coefficients ( $\alpha=0.1$  and 1). The  
30 background blue shade shows the 25%-75% percentiles of observed in-cloud ice number  
31 concentrations compiled by Krämer et al. (2009). The solid curves show the 50% percentiles  
32 of simulated ice number concentrations for each 1K bin and the error bars show the 25%-75%

1 percentiles. The model results were sampled every 3 hours from 30 S to 75 N over tropical,  
2 mid-latitude and Arctic regions which include the observation locations reported in Krämer et  
3 al. (2009). Fig. 3a shows that the HOM case overestimates the ice number concentrations by  
4 more than one order of magnitude in cirrus clouds at temperatures less than 205K but agrees  
5 better with observations in the temperature range from 205K to 220K. When the effect of  
6 vapour deposition onto pre-existing ice is included, the effective WGRID (0-5 cm s<sup>-1</sup>) is  
7 smaller than the original WGRID (0-15 cm s<sup>-1</sup>) for the grids with homogeneous freezing only  
8 (see Fig. 1b). Since a smaller updraft velocity translates into a slower increase of RH<sub>i</sub> with  
9 time, fewer newly formed ice particles from homogeneous freezing are needed to reverse the  
10 growth of RH<sub>i</sub> and thus stall the further formation of particles from homogeneous freezing.  
11 In fact, if the number of pre-existing ice particles is large enough, homogeneous freezing  
12 may not even occur. As a result, the ice number concentration in the HOM+PRE case (blue  
13 curve) is substantially smaller than that from the HOM case, especially at lower temperatures  
14 (more than one order of magnitude). This case matches the observations of ice number  
15 concentration pretty well at temperatures less than 205K, but underestimates concentrations at  
16 temperatures higher than 205K. Fig. 3b shows the results using a larger water vapour  
17 accommodation coefficient ( $\alpha=1$ ). Since ice particles grow faster with the larger water vapour  
18 accommodation coefficient, the RH<sub>i</sub> grows more slowly. So fewer ice particles are formed.  
19 For the HOM case, the ice number concentrations are much smaller at lower temperatures  
20 (compare black curves in Figure 3a and 3b). Case HOM+PRE (blue curves) also shows fewer  
21 ice particles but the difference between the case with  $\alpha=0.1$  and 1.0 is relatively smaller.

22 Fig 3c shows the results from the cases that include the competition between  
23 homogeneous and heterogeneous nucleation. Compared to the HOM case in Fig 3a, the  
24 COMP case in Fig 3c shows smaller ice number concentrations, which is expected since the  
25 competition from heterogeneous nucleation, which can occur at lower RH<sub>i</sub>, reduces the  
26 occurrence frequencies of homogeneous freezing. The much larger concentrations of  
27 homogeneous freezing haze particles (see Fig. 2a) typically allow more ice to form than  
28 heterogeneous nucleation. When 0.1% of SOA number is added as IN (case COMP+SOA01),  
29 there is a further reduction in the ice number concentration, especially at lower temperatures.  
30 But at higher temperatures ( $T>205K$ ) the change is relatively smaller. This is because at  
31 higher temperatures ( $T>205K$ ) ice grows faster than at lower temperatures thus the effect of  
32 any additional IN (SOA IN here) is diminished. When vapour deposition onto pre-existing ice  
33 is included (case COMP+PRE), the effect on ice number is much larger than the case for the

1 addition of SOA IN. The predicted ice number concentrations in this case are of the order of  
2  $10 \text{ L}^{-1}$ , which is comparable to the SOA IN number (about  $10 \text{ L}^{-1}$  as shown in Fig. 2c). The  
3 SOA IN require an RH<sub>i</sub> of about 120% to nucleate and start to consume the water vapour,  
4 while the pre-existing ice particles, if present, can start to consume the excess water vapour as  
5 long as the RH<sub>i</sub> is above 100%. So the pre-existing ice particles are more effective at reducing  
6 the RH<sub>i</sub> and suppressing ice nucleation by homogeneous and/or heterogeneous nucleation. In  
7 case COMP+PRE, since the effective WGRID is small, homogeneous freezing is almost  
8 completely suppressed. Further adding SOA IN to case COMP+PRE+SOA01 only decreases  
9 the ice number at the coldest temperatures ( $<195\text{K}$ ). When a larger water vapor  
10 accommodation coefficient ( $\alpha=1$ ) is used (Fig 3d), SOA IN are more effective at reducing the  
11 ice number at the coldest temperatures (see the pink curve at  $T<195\text{K}$  in Fig 3d) but become  
12 less important when vapour deposition onto pre-existing ice is included.

13 All in all, for cases using the large-scale grid resolved updraft velocity, as long as vapour  
14 deposition onto pre-existing ice is included, both the homogeneous freezing only case (HOM)  
15 and the competition cases (COMP) can produce in-cloud ice numbers in good agreement with  
16 the observations in the TTL cirrus clouds at temperatures less than 205K. If vapour deposition  
17 onto pre-existing ice during ice nucleation is not considered, then a larger water vapour  
18 accommodation coefficient ( $\alpha=1$ ) together with SOA as IN can also lead to a good agreement  
19 with observations. One caveat regarding the above results is that since the dynamical region  
20 studied in Spichtinger and Krämer (2013) was for very special conditions (namely it is  
21 characterized by very low vertical updrafts ( $< 2 \text{ cm s}^{-1}$ ), low temperatures ( $T<205\text{K}$ ) and  
22 strong stratification (i.e. high Brunt-Väisälä frequency)), the use of the large-scale grid  
23 resolved updraft velocity may not be valid for weaker stratifications or when WGRID is not  
24 small enough.

### 25 **3.3 Results from WGARY cases**

26 Figure 4 shows the results from the cases that include homogeneous/heterogeneous  
27 competition using WGARY as the sub-grid scale updraft velocity in the ice nucleation  
28 parameterization. Caution is needed in interpreting these results. Due to the possible  
29 underestimate of subgrid updraft velocities in the upper troposphere when using WGARY (as  
30 discussed in Section 3.1) and its oversimplified fitting which does not take into account the  
31 time-varying state of the atmosphere, this scheme might be considered a somewhat weaker  
32 parameterization than one that accounts for the full variability of the background atmospheric

1 | state. As a result, the simulated ice numbers are only statistically meaningful for mean climate  
2 | states. Results from the COMP case compare well with the observations in warm cirrus  
3 | clouds in the temperature range from 205K to 220K for both water vapour accommodation  
4 | coefficients. However, these cases overestimate number concentrations at temperatures less  
5 | than 205K. Similar to the results in Fig. 3, including vapour deposition onto pre-existing ice  
6 | can effectively reduce the in-cloud ice number concentrations. This leads to underestimated  
7 | ice number concentrations in warmer cirrus. But unlike the results from the WGRID cases in  
8 | Fig. 3, for this intermediate range updraft velocity (WGARY from 0.05-0.15 m s<sup>-1</sup> in Fig. 1),  
9 | the inclusion of vapour deposition onto pre-existing ice alone is not able to explain the  
10 | observed low ice number concentrations in cold cirrus clouds (T<205K). Adding SOA IN (red  
11 | curves in Fig. 4) further reduces the in-cloud ice number concentrations at the lowest  
12 | temperatures especially if  $\alpha=1$ . Adding SOA without including pre-existing ice (pink curves  
13 | in Fig. 4) is not very effective at the lowest temperatures unless  $\alpha=1$ . The best prediction of  
14 | ice number concentrations in cold cirrus clouds (T<205K) is from case COMP+PRE+SOA01  
15 | (red curve in Fig. 4b) when the effects from the pre-existing ice particles, a larger water vapor  
16 | accommodation coefficient ( $\alpha=1$ ) and SOA IN are all included. At higher temperatures  
17 | (T>210K) there is a slight increase of ice number concentration when adding SOA in the pre-  
18 | existing ice case, which suggests heterogeneous nucleation already dominates in this  
19 | temperature regime, so that the addition of SOA IN acts to increase ice numbers.

### 20 | **3.4 Results from WTKE cases**

21 | Figure 5 shows the results from cases with both heterogeneous and homogenous  
22 | nucleation (COMP) when the updraft velocity (WTKE) is based on the sub-grid scale  
23 | turbulent kinetic energy. As WTKE is on average much higher than the other two velocity  
24 | cases, the COMP cases without vapour deposition onto pre-existing ice overestimate the ice  
25 | numbers substantially for both water vapor accommodation coefficients. Adding SOA IN has  
26 | almost no effect on the simulated ice number concentrations except at higher temperatures  
27 | around 220K (pink curve in Fig. 5a). The critical IN number needed to suppress homogeneous  
28 | freezing increases with decreased temperature and increased updraft velocities. This suggests  
29 | that when WTKE is used, the addition of 0.1% of the total SOA as IN is not large enough to  
30 | reach this critical IN number (except at some of the temperatures higher than 215K) (see  
31 | pink curve in Fig. 5a). If 1% of the total SOA is allowed to act as IN, then there are  
32 | significant decreases in the ice number concentrations at temperatures above 205K (see pink

1 curves in Fig. S1). But the effect is still small at the lowest temperatures. When vapor  
2 deposition onto pre-existing ice is included, the WTKE is reduced but is still quite large  
3 compared to WGARY (see Fig. 1b). The simulated ice numbers from the COMP+PRE case  
4 are reduced by almost one order of magnitude and compare well with observations in cirrus  
5 clouds at temperatures warmer than 205K for both water vapour accommodation coefficients.  
6 Since the effective WTKE is smaller than the original WTKE, SOA IN are able to reduce  
7 some of the occurrences of homogenous freezing at temperatures as low as 205K (see red  
8 curve in Fig. 5a). But overall the effect from the added SOA IN is small and not effective in  
9 reducing the ice number concentration for these larger updraft velocities. Similar results  
10 have been reported in a geoengineering study by Penner et al. (2015) when WTKE is used  
11 and 0.1% or 0.5% of total SOA is added as IN (see their Fig. 2).

12

#### 13 **4 Conclusion and Discussion**

14 In this study, we examined the effect from three different updraft velocities and two  
15 different water vapor accommodation coefficients ( $\alpha=0.1$  or 1) used in ice nucleation  
16 parameterizations. We also examined the effect of including vapour deposition onto pre-  
17 existing ice particles during ice nucleation and the effect of including SOA as heterogeneous  
18 IN. The different simulations were compared to observed in-cloud ice number concentrations  
19 in cirrus clouds. The simulated in-cloud ice number is shown to strongly depend on the  
20 magnitude of the updraft velocity since this determines the occurrence frequency of  
21 homogenous freezing. Inclusion of vapour deposition onto pre-existing ice during nucleation  
22 or increasing the water vapor accommodation coefficient (from 0.1 to 1) can both effectively  
23 reduce the simulated ice numbers. The effect from SOA acting as IN is more complex since it  
24 depends on the background ice nucleation mechanism and whether or not the effect of pre-  
25 existing ice is included. Overall, SOA IN are most effective at suppressing homogenous  
26 freezing and thus reducing ice numbers when updraft velocities are intermediate in magnitude  
27 (e.g. WGARY from 0.05-0.15 m s<sup>-1</sup>). Including the effect of pre-existing ice reduces the effect  
28 of SOA IN. For small updraft velocities (e.g. WGRID), SOA IN are effective at reducing ice  
29 numbers only at lower temperatures. For large updraft velocities (e.g. WTKE), SOA IN only  
30 show a small effect at higher temperatures.

31 Here is a summary of the set-ups for different updraft velocities needed to produce ice  
32 number concentrations in-line with observations at temperatures less than 205K:

- 1       1) For the small grid resolved updraft velocities (i.e., case WGRID where  $W$  is typically  
2        $< 0.1 \text{ m s}^{-1}$ ), using either homogenous freezing only or including the competition  
3       between homogeneous and heterogeneous nucleation in the ice nucleation  
4       parameterization is able to produce the observed lower ice numbers when vapour  
5       deposition onto pre-existing ice particles is considered. When vapour deposition onto  
6       pre-existing ice particles is not considered, then a larger water vapour accommodation  
7       coefficient ( $\alpha=1$ ) and SOA IN are both needed to produce the observed lower ice  
8       numbers.
- 9       2) For intermediate velocities (e.g., WGARY with  $W$  varying from  $0.05\text{-}0.15 \text{ m s}^{-1}$ ), the  
10       effects from vapour deposition onto pre-existing ice particles, a larger water vapour  
11       accommodation coefficient ( $\alpha=1$ ), and SOA IN are all needed to produce the  
12       observed lower ice numbers.
- 13       3) For the larger updraft velocities (such as those found in WTKE which vary up to  $2 \text{ m}$   
14        $\text{s}^{-1}$ ), all set-ups overestimate the in-cloud ice numbers.

15       Thus, from our study, one can only use WGRID and WGARY to reproduce in-cloud ice  
16       numbers in-line with observations at temperatures less than 205K. But these simulations  
17       underestimate the ice number at temperatures higher than 205K. On the other hand, even  
18       though no set-up for WTKE is able to reproduce in-cloud ice numbers in-line with  
19       observations at temperatures less than 205K, the results agree best with observations at  
20       temperatures higher than 205K. No simple tuning of the ice nucleation parameters or set-up  
21       can form ice number concentrations that fit both temperature ranges. The obvious issue is that  
22       ice numbers from the model and the observations have nearly opposite temperature  
23       dependence slopes (i.e., decreased ice number with increased temperature seen from models  
24       vs. increased ice number with increased temperature seen from observations), a point noted  
25       previously using parcel model studies (Murphy 2014). The slope seen from the model results  
26       is a fundamental consequence of slower growth rate of ice particles and less water vapour  
27       available at lower temperatures. The only way to reverse the slope would be if some  
28       parameters, such as IN concentrations or sub-grid updraft velocity, were themselves functions  
29       of temperature. It is possible that CAM5 may overestimate the TKE in the upper troposphere  
30       at temperatures less than 205K, but an analysis of this is beyond the scope of this paper.  
31       When we use WGRID at temperatures lower than 205K and WTKE at temperatures higher  
32       than 205K, we are able to reverse the slope and the simulated ice number concentrations fit

1 the observations well in both temperature ranges (see Fig. 6a). But this choice of updraft  
2 velocity lacks any theory or observational support. It might be that we could only apply the  
3 proposal by Spichtinger and Krämer (2013) of using the large-scale updraft in the ice  
4 nucleation parameterization at temperatures lower than 205K but not at temperatures higher  
5 than 205K. The dynamic conditions near the top of troposphere may favour a combination of  
6 a slow persistent large-scale updraft velocity and short gravity waves which satisfy the special  
7 situation described by Spichtinger and Krämer (2013) in which the ice number formed from  
8 the short gravity waves is limited; while at lower altitudes, short gravity waves effect may not  
9 be limited due to higher large-scale updraft velocities. Another possibility might be that SOA  
10 number concentrations only become glassy and act as IN at temperatures less than 205K.  
11 However, while this model setup allows us to improve the prediction of crystal concentrations  
12 below 205K, it does not produce a reversed slope. Since the dynamical regime studied in  
13 Spichtinger and Krämer (2013) is characterized by a strong increasing stratification (i.e. high  
14 Brunt-Väisälä frequency) which coincides with the decreasing low temperatures ( $T < 205\text{K}$ )  
15 near the TTL, a more physical criterion would be using the modelled Brunt-Väisälä frequency  
16 ( $N$ ) to split the different regimes (WGRID vs. WTKE). Fig. 6b shows the simulated in-cloud  
17 ice numbers when using WGRID for  $N \leq 0.1 \text{ s}^{-1}$  and WTKE for  $N > 0.1 \text{ s}^{-1}$ . The critical  
18 value,  $N = 0.1 \text{ s}^{-1}$ , occurs around the altitude where the annually and zonally averaged  
19  $T=205\text{K}$  in the tropics. The simulated in-cloud ice number at  $T < 205\text{K}$  improves but not as  
20 much as that in Fig 6a in which the critical value of  $T$  (205K) is used. This is likely because  
21 the altitude at which  $N = 0.1 \text{ s}^{-1}$  does not necessarily coincide with the altitude at which  
22  $T=205\text{K}$  at any given time step in the model.

23

24

## 25 **Acknowledgements**

26 | [We thank the two anonymous reviewers and the editor who greatly helped improve this work.](#)

27 This work was supported by the NSF under grants AGS-0946739 and AGS-1540954. We  
28 acknowledge high-performance computing support from Yellowstone  
29 (<http://n2t.net/ark:/85065/d7wd3xhc>) provided by NCAR's Computational and Information  
30 Systems Laboratory and sponsored by the National Science Foundation.

31

## 1 **References**

- 2       Abbatt, J. P. D., Benz, S., Cziczo, D. J., Kanji, Z., Lohmann, U., and Möhler, O.: Solid  
3               ammonium sulfate aerosols as ice nuclei: a pathway for cirrus cloud formation,  
4               *Science*, 313, 1770–1773, doi:10.1126/science.1129726, 2006.
- 5       Barahona, D. and Nenes, A.: Parameterization of cirrus formation in large scale models:  
6               Homogenous nucleation, *J. Geophys. Res.*, 113, D11211,  
7               doi:10.1029/2007JD009355, 2008.
- 8       Barahona, D. and Nenes, A.: Parameterizing the competition between homogeneous and  
9               heterogeneous freezing in ice cloud formation – polydisperse ice nuclei, *Atmos.*  
10              *Chem. Phys.*, 9, 5933-5948, doi:10.5194/acp-9-5933-2009, 2009.
- 11       Barahona, D. and Nenes, A.: Dynamical states of low temperature cirrus, *Atmos. Chem.*  
12              *Phys.*, 11, 3757-3771, doi:10.5194/acp-11-3757-2011, 2011.
- 13       [Bretherton, C. S., and Park, S.: A new moist turbulence parameterization in the](#)  
14       [community atmosphere model, \*J. Climate\*, 22, 3422–3448, 2009.](#)
- 15       Chen, T., Rossow, W. B., and Zhang, Y.: Radiative effects of cloud-type variations. *J.*  
16              *Clim.*13, 264-286, 2000.
- 17       Cziczo, D. J., Froyd, K. D., Hoose, C., Jensen, E. J., Diao, M., Zondlo, M. A., Smith, J.  
18              B., Twohy, C. H., and Murphy, D. M.: Clarifying the Dominant Sources and  
19              Mechanisms of Cirrus Cloud Formation, *Science*, 340, 1320–1324,  
20              doi:10.1126/science.1234145, 2013.
- 21       Diao, M., Zondlo, M. A., Heymsfield, A. J., Beaton, S. P., and Rogers, D. C.: Evolution of  
22              ice crystal regions on the microscale based on in situ observations, *Geophys. Res.*  
23              *Lett.*, 40, 3473–3478, doi:10.1002/grl.50665, 2013.
- 24
- 25       Diao, M., Zondlo, M. A., Heymsfield, A. J., and Beaton, S. P.: Hemispheric comparison  
26              of cirrus cloud evolution using in situ measurements in HIAPER Pole-to-Pole  
27              Observations, *Geophys. Res. Lett.*, 41, 4090–4099,  
28              doi:10.1002/2014GL059873,2014.
- 29



1 Diao, M., Beaton, S. P., Pan, L. L., Homeyer, C. R., Honomichl, S., Bresch, J. F. and  
2 Bansemer A.: Distributions of ice supersaturation and ice crystals from airborne  
3 observations in relation to upper tropospheric dynamical boundaries, *J. Geophys.*  
4 *Res. Atmos.*, 120, 5101–5121, doi:10.1002/2015JD023139, 2015.

5 Dinh, T., Podglajen, A., Hertzog, A., Legras, B., and Plougonven, R.: Effect of gravity  
6 wave temperature fluctuations on homogeneous ice nucleation in the tropical  
7 tropopause layer, *Atmos. Chem. Phys. Discuss.*, 15, 8771-8799, doi:10.5194/acpd-  
8 15-8771-2015, 2015.

9 Field, P. R., Möhler, O., Connolly, P., Krämer, M., Cotton, R., Heymsfield, A. J.,  
10 Saathoff, H., and Schnaiter, M.: Some ice nucleation characteristics of Asian and  
11 Saharan desert dust, *Atmos. Chem. Phys.*, 6, 2991-3006, doi:10.5194/acp-6-2991-  
12 2006, 2006.

13 Gary, B. L.: Mesoscale temperature fluctuations in the stratosphere, *Atmos. Chem. Phys.*,  
14 6, 4577-4589, doi:10.5194/acp-6-4577-2006, 2006.

15 Gary, B. L.: Mesoscale temperature fluctuations in the Southern Hemisphere stratosphere,  
16 *Atmos. Chem. Phys.*, 8, 4677-4681, doi:10.5194/acp-8-4677-2008, 2008.

17 Gettelman, A., Liu, X., Ghan, S. J., Morrison, H., Park, S., Conley, A. J., Klein, S. A.,  
18 Boyle, J., Mitchell, D. L., and Li, J. L. F.: Global simulations of ice nucleation and  
19 ice supersaturation with an improved cloud scheme in the Community Atmosphere  
20 Model, *J. Geophys. Res.-Atmos.*, 115, D18216, doi:10.1029/2009jd013797, 2010.

21 Gettelman, A., Liu, X., Barahona, D., Lohmann, U., and Chen, C.: Climate impacts of ice  
22 nucleation, *J. Geophys. Res.-Atmos.*, 117, D20201, doi:10.1029/2012jd017950,  
23 2012.

24 Hoose, C. and Möhler, O.: Heterogeneous ice nucleation on atmospheric aerosols: a  
25 review of results from laboratory experiments, *Atmos. Chem. Phys.*, 12, 9817-  
26 9854, doi:10.5194/acp-12-9817-2012, 2012.

27 IPCC, 2013: Climate Change 2013: The Physical Science Basis. Contribution of Working  
28 Group I to the Fifth Assessment Report of the Intergovernmental Panel on Climate  
29 Change [Stocker, T.F., D. Qin, G.-K. Plattner, M. Tignor, S.K. Allen, J. Boschung,  
30 A. Nauels, Y. Xia, V. Bex and P.M. Midgley (eds.)]. Cambridge University Press,  
31 Cambridge, United Kingdom and New York, NY, USA, 1535 pp.

- 1 Jensen, E. J., Toon, O. B., Selkirk, H. B., Spinhirne, J. D., and Schoeberl, M. R.: On the  
2 formation and persistence of subvisible cirrus clouds near the tropical tropopause,  
3 *J. Geophys. Res.*, 101, 21361–21375, 1996.
- 4 Jensen, E. J., Pfister, L., Bui, T.-P., Lawson, P., and Baumgardner, D.: Ice nucleation and  
5 cloud microphysical properties in tropical tropopause layer cirrus, *Atmos. Chem.*  
6 *Phys.*, 10, 1369-1384, doi:10.5194/acp-10-1369-2010, 2010.
- 7 Jensen, E. J., Pfister, L., and Bui T. P.: Physical processes controlling ice concentrations  
8 in cold cirrus near the tropical tropopause, *J. Geophys. Res.*, 117, D11205,  
9 doi:10.1029/2011JD017319, 2012.
- 10 Jensen, E. J., Diskin, G., Lawson, R. P., Lance, S., Bui, T. P., Hlavka, D., McGill, M.,  
11 Pfister, L., Toon, O. B., and Gao, R.: Ice nucleation and dehydration in the  
12 Tropical Tropopause Layer, *P. Natl. Acad. Sci.*, 110, 2041–2046,  
13 doi:10.1073/pnas.1217104110, 2013.
- 14 K ärcher, B. and Str öm, J.: The roles of dynamical variability and aerosols in cirrus cloud  
15 formation, *Atmos. Chem. Phys.*, 3, 823-838, doi:10.5194/acp-3-823-2003, 2003.
- 16 K ärcher, B., Hendricks, J., and Lohmann, U.: Physically based parameterization of cirrus  
17 cloud formation for use in global atmospheric models, *J. Geophys. Res.*, 111,  
18 D01205, doi: 10.1029/2005JD006219, 2006.
- 19 K ärcher, B. and Burkhardt, U.: A cirrus cloud scheme for general circulation models,  
20 *Quart. J. Roy. Meteor. Soc.*, 134, 1439–1461, doi:10.1002/Qj.301, 2008.
- 21 Kay, J. E., and Wood, R.: Timescale analysis of aerosol sensitivity during homogeneous  
22 freezing and implications for upper tropospheric water vapor budgets, *Geophys.*  
23 *Res. Lett.*, 35, L10809, doi:10.1029/2007gl032628, 2008.
- 24 Koehler, K. A., DeMott, P. J., Kreidenweis, S. M., Popovicheva, O. B., Petters, M. D.,  
25 Carrico, C. M., Kireeva, E. D., Khokhlovac, T. D., and Shonijac, N. K.: Cloud  
26 condensation nuclei and ice nucleation activity of hydrophobic and hydrophilic  
27 soot particles, *Phys. Chem. Chem. Phys.*, 11, 7906–7920, doi:10.1039/b905334b,  
28 2009.
- 29 Koop, T., Luo, B., Tsias, A., and Peter, T.: Water activity as the determinant for  
30 homogeneous ice nucleation in aqueous solutions, *Nature*, 406, 611–614, 2000.

1 Kr ämer, M., Schiller, C., Afchine, A., Bauer, R., Gensch, I., Mangold, A., Schlicht, S.,  
2 Spelten, N., Sitnikov, N., Borrmann, S., de Reus, M., and Spichtinger, P.: Ice  
3 supersaturations and cirrus cloud crystal numbers, *Atmos. Chem. Phys.*, 9, 3505-  
4 3522, doi:10.5194/acp-9-3505-2009, 2009.

5 Kuebbeler, M., Lohmann, U., Hendricks, J., and K ärcher, B.: Dust ice nuclei effects on  
6 cirrus clouds, *Atmos. Chem. Phys.*, 14, 3027-3046, doi:10.5194/acp-14-3027-2014, 2014.

7 Lin, G., Penner, J. E., Sillman, S., Taraborrelli, D., and Lelieveld, J.: Global modeling of  
8 SOA formation from dicarbonyls, epoxides, organic nitrates and peroxides,  
9 *Atmos. Chem. Phys.*, 12, 4743-4774, doi:10.5194/acp-12-4743-2012, 2012.

10 Lin, G., Sillman, S., Penner, J. E., and Ito, A.: Global modeling of SOA: the use of  
11 different mechanisms for aqueous-phase formation, *Atmos. Chem. Phys.*, 14,  
12 5451-5475, doi:10.5194/acp-14-5451-2014, 2014.

13 Liu, X. and Penner, J. E.: Ice nucleation parameterization for a global model,  
14 *Meteorologische Zeitschrift*, 14(4), 499–514, 2005.

15 Liu, X., Penner, J. E., Ghan, S. J., and Wang, M.: Inclusion of ice microphysics in the  
16 NCAR community atmospheric model version 3 (CAM3), *J. Climate*, 20, 4526–  
17 4547, doi: 10.1175/JCLI4264.1, 2007.

18 Liu, X., Easter, R. C., Ghan, S. J., Zaveri, R., Rasch, P., Shi, X., Lamarque, J.-F.,  
19 Gettelman, A., Morrison, H., Vitt, F., Conley, A., Park, S., Neale, R., Hannay, C.,  
20 Ekman, A. M. L., Hess, P., Mahowald, N., Collins, W., Iacono, M. J., Bretherton,  
21 C. S., Flanner, M. G., and Mitchell, D.: Toward a minimal representation of  
22 aerosols in climate models: description and evaluation in the Community  
23 Atmosphere Model CAM5, *Geosci. Model Dev.*, 5, 709-739, doi:10.5194/gmd-5-  
24 709-2012, 2012a.

25 Liu, X., Shi, X., Zhang, K., Jensen, E. J., Gettelman, A., Barahona, D., Nenes, A., and  
26 Lawson, P.: Sensitivity studies of dust ice nuclei effect on cirrus clouds with the  
27 Community Atmosphere Model CAM5, *Atmos. Chem. Phys.*, 12, 12061-12079,  
28 doi:10.5194/acp-12-12061-2012, 2012b.

29 Magee, N., Moyle, A. M., and Lamb, D.: Experimental determination of the deposition  
30 coefficient of small cirrus-like ice crystals near ?50 C, *Geophys. Res. Lett.*, 33,  
31 L17813, doi:10.1029/2006GL026665, 2006.

- 1 Meyers, M. P., DeMott, P. J., and Cotton, R.: New primary ice nucleation  
2 parameterization in an explicit cloud model, *J. Appl. Meteorol.*, 31, 708–721,  
3 1992.
- 4 Möhler, O., Büttner, S., Linke, C., Schnaiter, M., Saathoff, H., Stetzer, O., Wagner, R.,  
5 Krämer, M., Mangold, A., Ebert, V., and Schurath, U.: Effect of sulfuric acid  
6 coating on heterogeneous ice nucleation by soot aerosol particles, *J. Geophys.*  
7 *Res.*, 110, D11210, doi:10.1029/2004JD005169, 2005.
- 8 Morrison, H., and Gettelman A., A new two-moment bulk stratiform cloud microphysics  
9 scheme in the Community Atmosphere Model, version 3 (CAM3). Part I:  
10 Description and numerical tests. *Journal of Climate*, 21, 3642-3659,  
11 doi:10.1175/2008JCLI2105.1, 2008.
- 12 Morrison, H., and Pinto J. O.: Mesoscale modeling of springtime arctic mixed-phase  
13 stratiform clouds using a new two-moment bulk microphysics scheme, *J. Atmos.*  
14 *Sci.*, 62, 3683–3704, 2005.
- 15 Murphy, D. M.: Rare temperature histories and cirrus ice number density in a parcel and a  
16 one-dimensional model, *Atmos. Chem. Phys.*, 14, 13013-13022, doi:10.5194/acp-  
17 14-13013-2014, 2014.
- 18 Murray, B., Wilson, T. W., Dobbie, S., Cui, Z., Al-Jumur, S. M. R. K., Möhler, O.,  
19 Schnaiter, M., Wagner, R., Benz, S., Niemand, M., Saathoff, H., Ebert, V.,  
20 Wagner, S., and Krächer, B.: Heterogeneous nucleation of ice particles on glassy  
21 aerosols under cirrus conditions, *Nat. Geosci.*, 3, 233–237,  
22 doi:10.1038/NGEO817, 2010.
- 23 Neale, R. B., Gettelman, A., Park, S., Conley, A. J., Kinnison, D., Marsh, D., Smith, A.  
24 K., Vitt, F., Morrison, H., Cameron-Smith, P., Collins, W. D., Iacono, M. J.,  
25 Easter, R. C., Liu, X., and Taylor, M. A.: Description of the NCAR Community  
26 Atmosphere Model (CAM 5.0), NCAR Tech. Note NCAR/TN-485CSTR, Natl.  
27 Cent. for Atmos. Res, Boulder, Co, 289 pp., 2012.
- 28 Penner, J. E., Zhou, C. and Liu, X.: Can cirrus cloud seeding be used for geoengineering?,  
29 *Geophys. Res. Lett.*, 42, 8775–8782, doi:10.1002/2015GL065992, 2015.

- 1 Phillips, V. T. J., Donner, L. J., and Garner, S. T.: Nucleation processes in deep  
2 convection simulated by a cloud-system-resolving model with double-moment  
3 bulk microphysics, *J. Atmos. Sci.*, 64, 738–761, doi:10.1175/JAS3869.1, 2007.
- 4 Phillips, V. T. J., DeMott, P. J., and Andronache, C.: An empirical parameterization of  
5 heterogeneous ice nucleation for multiple chemical species of aerosol, *J. Atmos.*  
6 *Sci.*, 65, 2757–2783, doi:10.1175/2007JAS2546.1, 2008.
- 7 [Podglajen, A., Hertzog, A., Plougonven, R., and Legras, B.: Lagrangian temperature and](#)  
8 [vertical velocity fluctuations due to gravity waves in the lower stratosphere,](#)  
9 [Geophys. Res. Lett., 43, 3543–3553, doi:10.1002/2016GL068148, 2016.](#)
- 10 Pratt, K., DeMott, P., French, J., Wang, Z., Westphal, D., Heyms-field, A., Twohy, C.,  
11 Prenni, A., and Prather, K.: In situ detection of biological particles in cloud ice-  
12 crystals, *Nature Geosci.*, 2, 398–401, 2009.
- 13 Pruppacher, H. R. and Klett, J. D.: *Microphysics of Clouds and Precipitation,*  
14 *Atmospheric and Oceanographic Sciences Library, Kluwer Academic Publishers,*  
15 *Dordrecht, The Netherlands, 1997.*
- 16 Ramanathan, V. and Collins, W.: Thermodynamic regulation of ocean warming by cirrus  
17 clouds deduced from observations of the 1987 El-Nino, *Nature*, 351, 27–32, 1991.
- 18 Rogers, D. C., DeMott, P. J., Kreidenweis, S. M. and Chen, Y.: Measurements of ice  
19 nucleating aerosols during SUCCESS, *Geophys. Res. Lett.*, 25, 1383–1386,  
20 doi:10.1029/97GL03478, 1998.
- 21 Rossow, W. B. and Schiffer, R. A.: Advances in understanding clouds from ISCCP, *Bull.*  
22 *Amer. Meteor. Soc.*, 80, 2261–2287, 1999.
- 23 Sassen, K., Wang Z., and Liu, D.: Global distribution of cirrus clouds from  
24 CloudSat/Cloud-Aerosol Lidar and Infrared Pathfinder Satellite Observations  
25 (CALIPSO) measurements, *J. Geophys. Res.*, 113, D00A12,  
26 doi:10.1029/2008JD009972, 2008.
- 27 Shi, X., Liu, X., and Zhang, K.: Effects of pre-existing ice crystals on cirrus clouds and  
28 comparison between different ice nucleation parameterizations with the  
29 Community Atmosphere Model (CAM5), *Atmos. Chem. Phys.*, 15, 1503-1520,  
30 doi:10.5194/acp-15-1503-2015, 2015.

- 1 Skrotzki, J., Connolly, P., Schnaiter, M., Saathoff, H., Möhler, O., Wagner, R., Niemand,  
2 M., Ebert, V., and Leisner, T.: The accommodation coefficient of water molecules  
3 on ice – cirrus cloud studies at the AIDA simulation chamber, *Atmos. Chem.*  
4 *Phys.*, 13, 4451-4466, doi:10.5194/acp-13-4451-2013, 2013.
- 5 Spichtinger, P. and Gierens, K. M.: Modelling of cirrus clouds – Part 2: Competition of  
6 different nucleation mechanisms, *Atmos. Chem. Phys.*, 9, 2319-2334,  
7 doi:10.5194/acp-9-2319-2009, 2009.
- 8 Spichtinger, P. and Krämer, M.: Tropical tropopause ice clouds: a dynamic approach to  
9 the mystery of low crystal numbers, *Atmos. Chem. Phys.*, 13, 9801-9818,  
10 doi:10.5194/acp-13-9801-2013, 2013.
- 11 Stubenrauch, C. J., Cros, S., Guignard, A., and Lamquin, N.: A 6-year global cloud  
12 climatology from the Atmospheric InfraRed Sounder AIRS and a statistical  
13 analysis in synergy with CALIPSO and CloudSat, *Atmos. Chem. Phys.*, 10, 7197-  
14 7214, doi:10.5194/acp-10-7197-2010, 2010. Wang, M. and Penner, J. E.: Cirrus  
15 clouds in a global climate model with a statistical cirrus cloud scheme, *Atmos.*  
16 *Chem. Phys.*, 10, 5449-5474, doi:10.5194/acp-10-5449-2010, 2010.
- 17 Wang, M., Liu, X., Zhang K., and Comstock J. M.: Aerosol effects on cirrus through ice  
18 nucleation in the Community Atmosphere Model CAM5 with a statistical cirrus  
19 scheme, *J. Adv. Model. Earth Syst.*, 6, 756–776, doi:10.1002/2014MS000339,  
20 2014.
- 21 Wang, P. H., Minnis, P., McCormick, M. P., Kent, G. S., and Skeens, K. M.: A 6-year  
22 climatology of cloud occurrence frequency from stratospheric aerosol and gas  
23 experiment II observations (1985-1990), *J. Geophys. Res.*, 101, 29407–29429,  
24 1996.
- 25 Wylie, D. P. and Menzel, W. P.: Eight years of high cloud statistics using HIRS, *J.*  
26 *Climate*, 12, 170–184, 1999.
- 27 Zhang, K., Liu, X., Wang, M., Comstock, J. M., Mitchell, D. L., Mishra, S., and Mace, G.  
28 G.: Evaluating and constraining ice cloud parameterizations in CAM5 using  
29 aircraft measurements from the SPARTICUS campaign, *Atmos. Chem. Phys.*, 13,  
30 4963-4982, doi:10.5194/acp-13-4963-2013, 2013.

1       Zhou, C., and Penner J. E.: Aircraft soot indirect effect on large-scale cirrus clouds: Is the  
2               indirect forcing by aircraft soot positive or negative?, *J. Geophys. Res. Atmos.*,  
3               119, doi:10.1002/2014JD021914, 2014.

4       Zhou, C., Penner, J. E., Flanner, M. G., Bisiaux, M. M., Edwards, R. and McConnell J.  
5               R.: Transport of black carbon to polar regions: Sensitivity and forcing by black  
6               carbon, *Geophys. Res. Lett.*, 39, L22804, doi:10.1029/2012GL053388, 2012b.

7       Zhou, C., Penner, J. E., Ming, Y., and Huang, X. L.: Aerosol forcing based on CAM5 and  
8               AM3 meteorological fields, *Atmos. Chem. Phys.*, 12, 9629-9652, doi:10.5194/acp-  
9               12-9629-2012, 2012a.

1

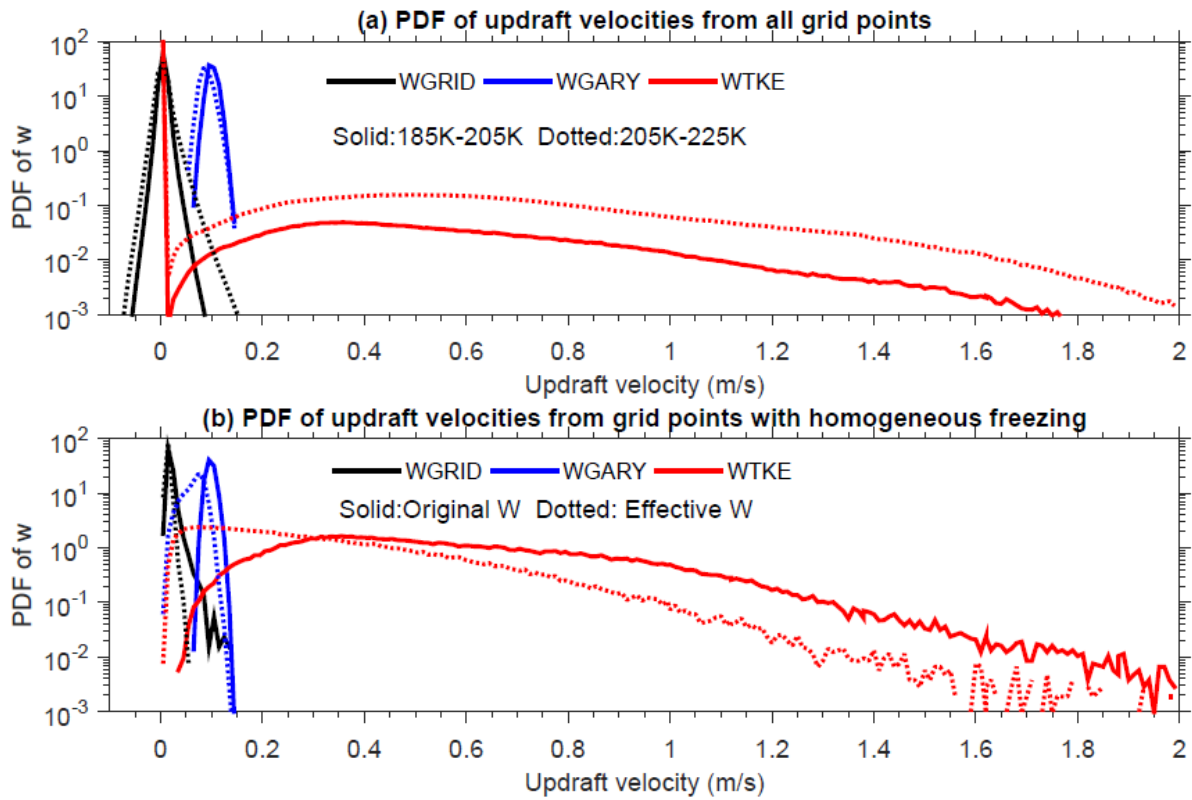
Table 1. Description of the experiments.

Case name	Case description
HOM*	Only homogeneous freezing in the ice nucleation parameterization.
HOM+PRE*	Only homogeneous freezing in the ice nucleation parameterization; pre-existing ice effect in the ice nucleation parameterization.
COMP	Competition between homogeneous freezing and heterogeneous nucleation.
COMP+SOA01	Competition between homogeneous freezing and heterogeneous nucleation; 0.1% of SOA acting as heterogeneous IN.
COMP+PRE	Competition between homogeneous freezing and heterogeneous nucleation; pre-existing ice effect in the ice nucleation parameterization.
COMP+PRE+SOA01	Competition between homogeneous freezing and heterogeneous nucleation; pre-existing ice effect in the ice nucleation parameterization; 0.1% of SOA acting as heterogeneous IN.

2

\* Case HOM and HOM+PRE are for WGRID only.

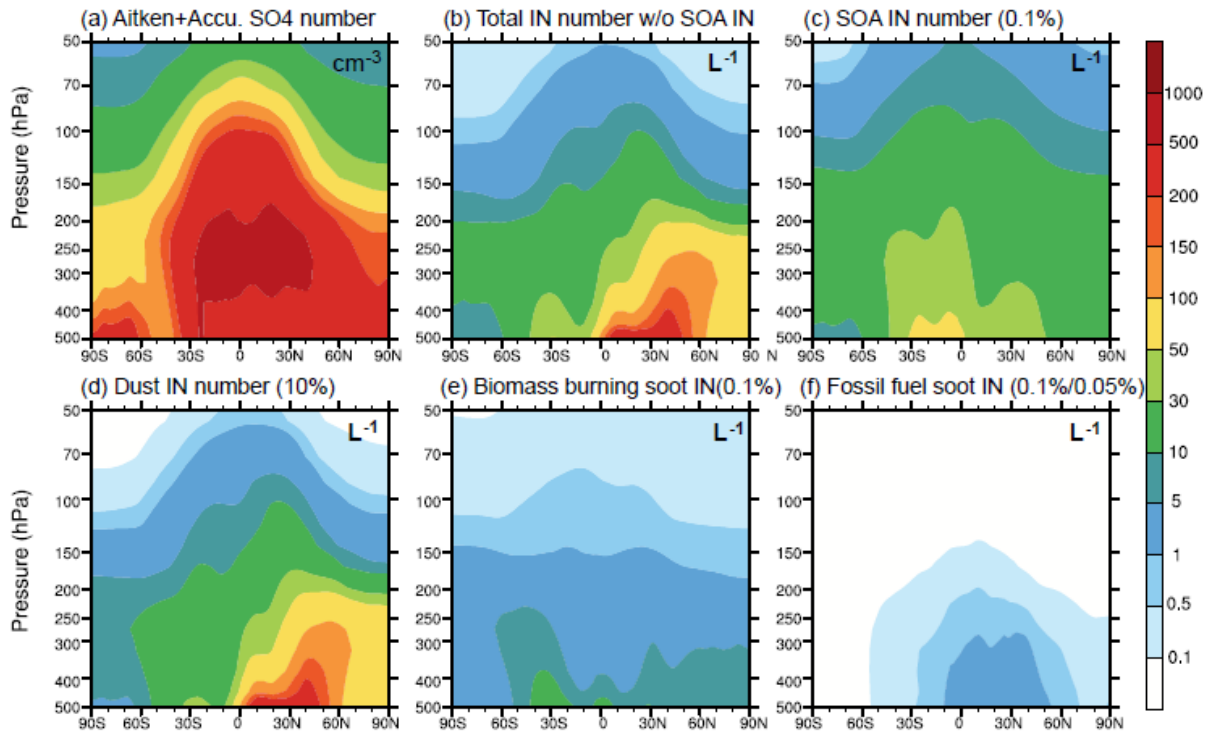




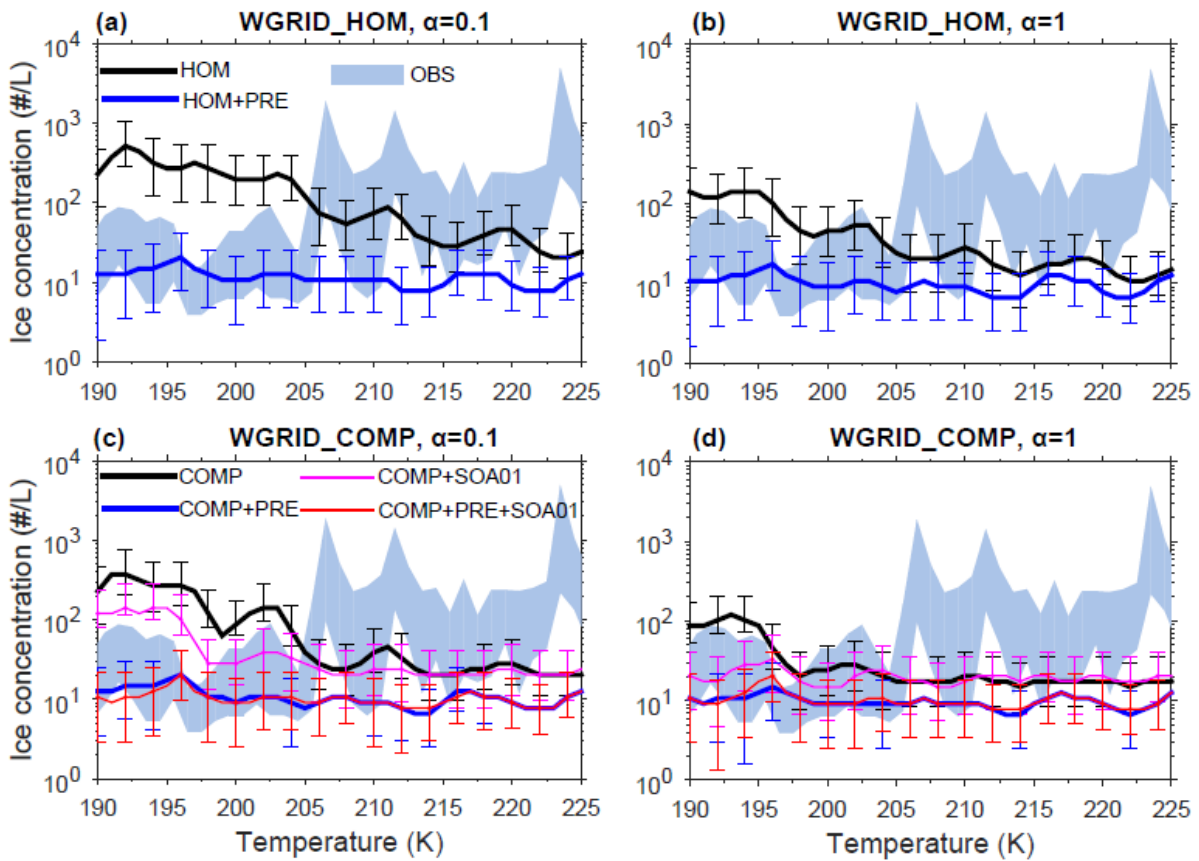
1

2 Figure 1 (a) Probability density functions (PDFs) of updraft velocity for three different  
 3 representations (black: large-scale W, blue: meso-scale W from Gary 2006, 2008, red: TKE  
 4 based subgrid W) from all grid points in two temperature ranges. (b) Probability density  
 5 functions of updraft velocity for the three different updraft velocity representations from grid  
 6 points with homogenous freezing only in the temperature range 185K-205K. Solid curves are  
 7 the original W and dotted curves are the effective W after accounting for vapour deposition  
 8 onto pre-existing ice. Model results are sampled every 3 hour below 87hPa.

9

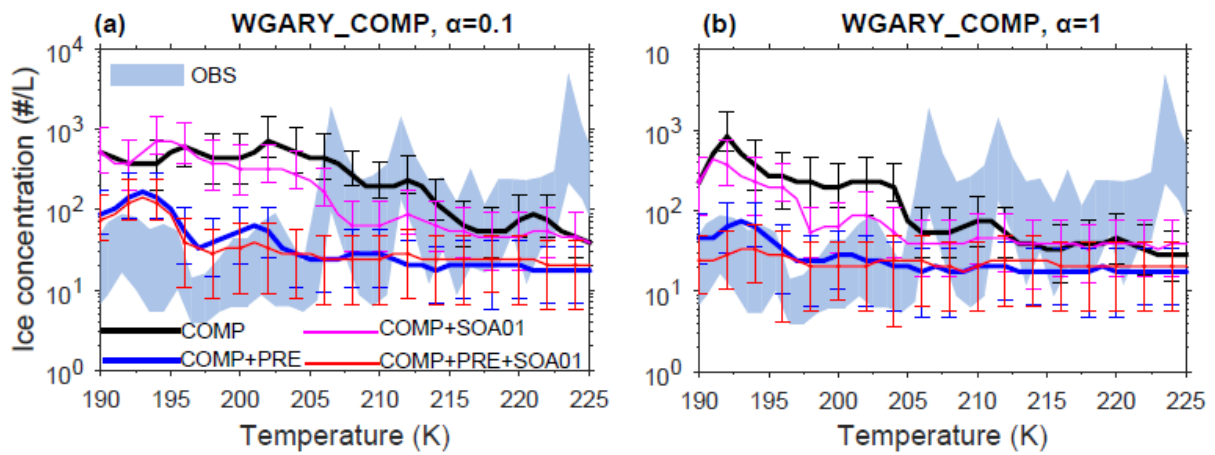


1  
 2 Figure 2 a) Aitken and accumulation mode sulfate number ( $\text{cm}^{-3}$ ). b) Total background  
 3 heterogeneous IN number ( $\text{L}^{-1}$ ) without SOA IN: i.e. the sum of panels d, e, and f. c) SOA IN  
 4 number ( $\text{L}^{-1}$ ): 0.1% of the total SOA number. d) Dust IN number ( $\text{L}^{-1}$ ): 10% of the total dust  
 5 number. e) Biomass burning soot IN number ( $\text{L}^{-1}$ ): 0.1% of total biomass burning soot number.  
 6 f) Fossil fuel soot IN number ( $\text{L}^{-1}$ ): 0.1% of hydrophilic fossil fuel soot and 0.05% of  
 7 hydrophobic fossil fuel soot.



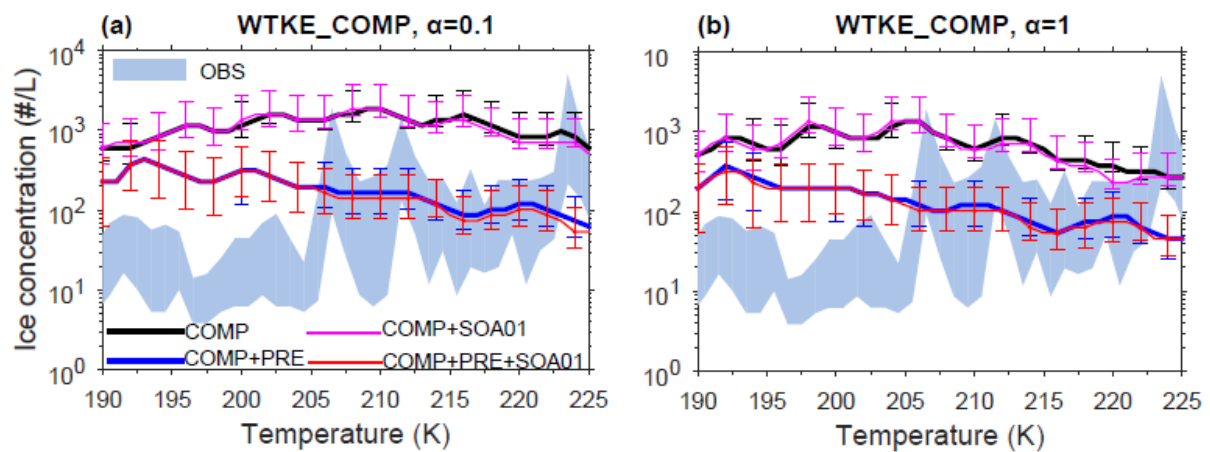
1

2 Figure 3 In-cloud ice crystal number concentration (#/L) versus temperature from cases using  
 3 the grid resolved updraft velocity (WGRID) in the ice nucleation parameterization. Solid lines  
 4 show the 50% percentile values for each 1K bin. Error bars show the 25%-75% percentiles.  
 5 Background shaded regions show the 25%-75% percentiles from observations compiled by  
 6 Krämer et al. (2009). Upper panel shows the results from the homogeneous freezing only  
 7 cases and bottom panel shows the results from the competition cases. Left panel shows the  
 8 results from cases with water vapor accommodation coefficient  $\alpha = 0.1$ . Right panel shows  
 9 the results from cases with water vapor accommodation coefficient  $\alpha = 1$ . Model results are  
 10 sampled every 3 hours from 30 S to 75 N over tropical, mid-latitude and Arctic regions which  
 11 includes the observation locations reported in Krämer et al. (2009).



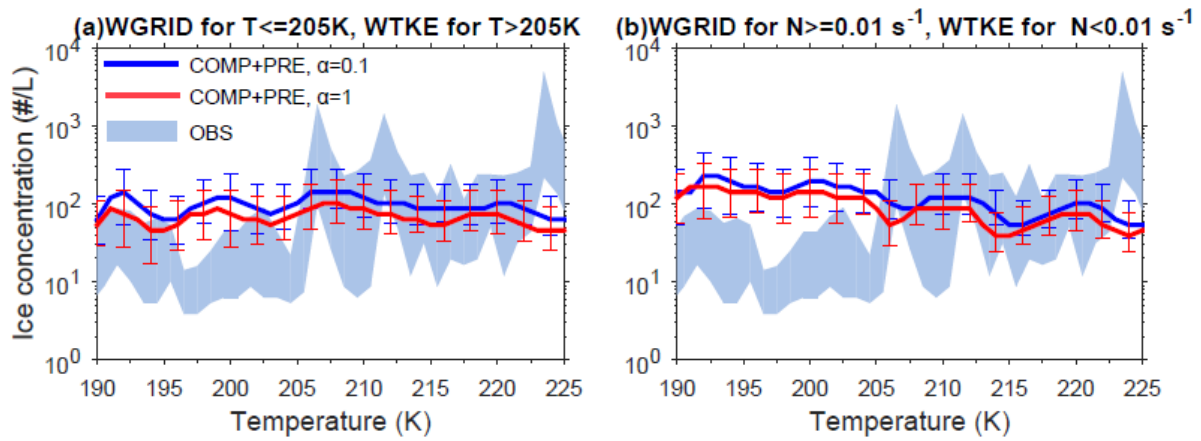
1  
 2 Figure 4 Same as Figure 3 (c) and (d) except the updraft velocity (WGARY) derived from the  
 3 observed meso-scale temperature fluctuations from Gary (2006, 2008) was used in the ice  
 4 nucleation parameterization.

5



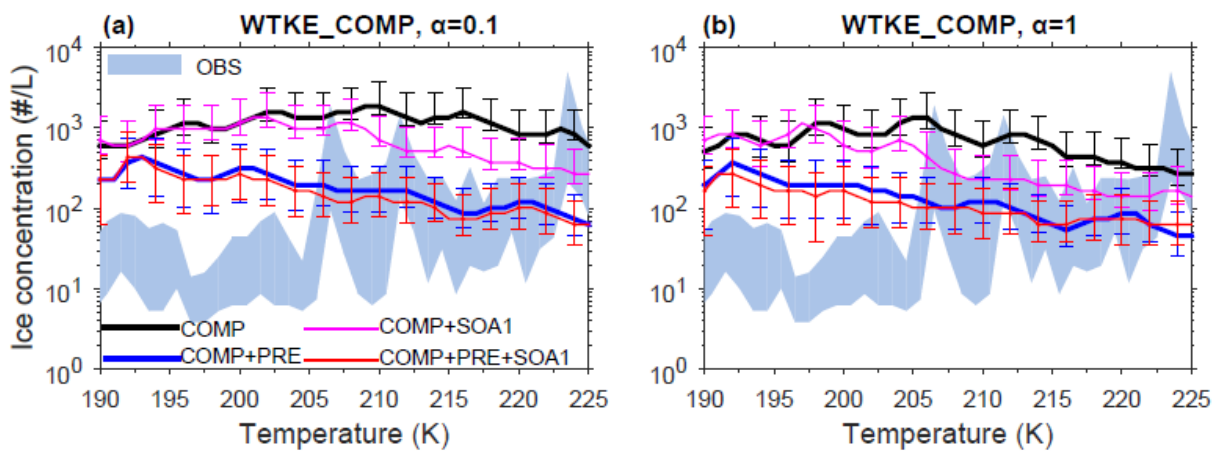
6  
 7 Figure 5 Same as Figure 3 (c) and (d) except the sub-grid scale turbulent kinetic energy based  
 8 updraft velocity (WTKE) was used in the ice nucleation parameterization.

9



1  
 2 Figure 6 In-cloud ice crystal number concentration (#/L) versus temperature from  
 3 COMP+PRE cases with a mixed use of WGRID and WTKE based on a critical temperature  
 4 or Brunt-Väsälä frequency. (left) WGRID for  $T \leq 205\text{K}$  and WTKE for  $T > 205\text{K}$ ; (right)  
 5 WGRID for the Brunt-Väsälä frequency  $N \geq 0.01 \text{ s}^{-1}$  and WTKE for  $N < 0.01 \text{ s}^{-1}$ . Blue curves  
 6 is-are from the case with water vapor accommodation coefficient  $\alpha = 0.1$  and the red curves  
 7 are from the case with water vapor accommodation coefficient  $\alpha = 1$ .

8



9

10 Figure S1 Same as Figure 5 except 1% of total SOA acting as IN.